each amplified product was calculated from two independent ChIP experiments and a total of four independent PCR analyses.

Enzyme-linked immunosorbent assay

To quantify the secretion of VASH2, an enzyme-linked immunosorbent assay kit (Huili Biotech, DZE11701, Changchun, China) was used to measure secreted VASH2. The samples analyzed were cell supernatants from HepG2-VASH2-SVBP and HepG2-VASH2 cells collected after 24, 48 or 72 h of culture. The cell numbers in each dish were counted to normalize the levels measured in the two groups. First, a standard was diluted to different concentrations to generate a standard curve. The supernatants were diluted sixfold with sample diluent and added to wells. After incubating at 37 °C for 30 min and washing five times, 50 μl horseradish peroxidase-conjugate reagents was added to each well except the blank. The plate was then incubated at 37 °C and washed as above. Chromogen Solution A and Chromogen Solution B (Huili Biotech, Changchun, China) were added to each well and incubated for 15 min in the dark. Finally, 50-μl stop solution was added to each well to stop the reaction. The optical density was read at 450 nm. The data are reported as concentration × 6/cell number (ng/ml/10^6 cells).

Coculture assay

HUVECs and HepG2 cells expressing different levels of VASH2 were cocultured using six-well modified Boyden chambers with 0.4 μm pores (Corning, 3412, New York, NY, USA). HepG2 cells were plated in the lower chambers and HUVECs were seeded in the upper chambers. After the cells adhered, the culture medium was changed to serum-free DMEM, and the upper chambers containing the HUVECs were transferred to the plates with HepG2 cells. After coculture for 24, 48 or 72 h, RNA was isolated from both the HepG2 cells and the HUVECs. The expression of the angiogenesis factors FGF-2, VEGF and VASH1 was analyzed. Primers are available on request.

Statistical analysis

All experiments were repeated in triplicate in this article. Where indicated statistical significance was determined by the Student's *t*-test. *P*-values <0.05 were considered as statistically significant.

CONFLICT OF INTEREST

The authors declare no conflict of interest.

ACKNOWLEDGEMENTS

We are very grateful to Professor Yujie Sun from Nanjing Medical University for continuous technical support. This work was supported by grants from the National Nature Science Foundation of China (no. 81172267 and 30901627).

REFERENCES

1 Semela D, Dufour JF. Angiogenesis and hepatocellular carcinoma. *J Hepatol* 2004; **41**: 864–880.
2 Eggert A, Ikegaki N, Kwiatkowski J, Zhao H, Brodeur GM, Himelstein BP. High-level expression of angiogenic factors is associated with advanced tumor stage in human neuroblastomas. *Clin Cancer Res* 2000; **6**: 1900–1908.
3 Doger FK, Meteoglu I, Tuncyurek P, Okyay P, Cevikel H. Does the EGFR and VEGF expression predict the prognosis in colon cancer? *Eur Surg Res* 2006; **38**: 540–544.
4 Cha HJ, Lee HH, Chae SW, Cho WJ, Kim YM, Choi HJ *et al.* Tristetraprolin down-regulates the expression of both VEGF and COX-2 in human colon cancer. *Hepatogastroenterology* 2011; **58**: 790–795.
5 Folkman J. Angiogenesis: an organizing principle for drug discovery? *Nat Rev Drug Discov* 2007; **6**: 273–286.
6 Llovet JM, Ricci S, Mazzaferro V, Hilgard P, Gane E, Blanc JF *et al.* Sorafenib in advanced hepatocellular carcinoma. *N Engl J Med* 2008; **359**: 378–390.
7 Zhu AX, Duda DG, Sahani DV, Jain RK. HCC and angiogenesis: possible targets and future directions. *Nat Rev Clin Oncol* 2011; **8**: 292–301.
8 Watanabe K, Hasegawa Y, Yamashita H, Shimizu K, Ding Y, Abe M *et al.* Vasohibin as an endothelium-derived negative feedback regulator of angiogenesis. *J Clin Invest* 2004; **114**: 898–907.
9 Yoshinaga K, Ito K, Moriya T, Nagase S, Takano T, Niikura H *et al.* Roles of intrinsic angiogenesis inhibitor, vasohibin, in cervical carcinomas. *Cancer Sci* 2011; **102**: 446–451.
10 Tamaki K, Moriya T, Sato Y, Ishida T, Maruo Y, Yoshinaga K *et al.* Vasohibin-1 in human breast carcinoma: a potential negative feedback regulator of angiogenesis. *Cancer Sci* 2009; **100**: 88–94.
11 Shibuya T, Watanabe K, Yamashita H, Shimizu K, Miyashita H, Abe M *et al.* Isolation and characterization of vasohibin-2 as a homologue of VEGF-inducible endothelium-derived angiogenesis inhibitor vasohibin. *Arterioscler Thromb Vasc Biol* 2006; **26**: 1051–1057.
12 Kimura H, Miyashita H, Suzuki Y, Kobayashi M, Watanabe K, Sonoda H *et al.* Distinctive localization and opposed roles of vasohibin-1 and vasohibin-2 in the regulation of angiogenesis. *Blood* 2009; **113**: 4810–4818.
13 Strahl BD, Allis CD. The language of covalent histone modifications. *Nature* 2000; **403**: 41–45.
14 Jenuwein T, Allis CD. Translating the histone code. *Science* 2001; **293**: 1074–1080.
15 Santos-Rosa H, Schneider R, Bannister AJ, Sherriff J, Bernstein BE, Emre NC *et al.* Active genes are tri-methylated at K4 of histone H3. *Nature* 2002; **419**: 407–411.
16 Plath K, Fang J, Mlynarczyk-Evans SK, Cao R, Worringer KA, Wang H *et al.* Role of histone H3 lysine 27 methylation in X inactivation. *Science* 2003; **300**: 131–135.
17 Gorisch SM, Wachsmuth M, Toth KF, Lichter P, Rippe K. Histone acetylation increases chromatin accessibility. *J Cell Sci* 2005; **118**(Part 24): 5825–5834.
18 Suzuki Y, Kobayashi M, Miyashita H, Ohta H, Sonoda H, Sato Y. Isolation of a small vasohibin-binding protein (SVBP) and its role in vasohibin secretion. *J Cell Sci* 2010; **123**(Part 18): 3094–3101.
19 Palacios D, Mozzetta C, Consalvi S, Caretti G, Saccone V, Proserpio V *et al.* TNF/p38alpha/polycomb signaling to Pax7 locus in satellite cells links inflammation to the epigenetic control of muscle regeneration. *Cell Stem Cell* 2010; **7**: 455–469.
20 Tammali R, Reddy AB, Srivastava SK, Ramana KV. Inhibition of aldose reductase prevents angiogenesis *in vitro* and *in vivo*. *Angiogenesis* 2011; **14**: 209–221.
21 Mi J, Zhang X, Liu Y, Reddy SK, Rabbani ZN, Sullenger BA *et al.* NF-kappaB inhibition by an adenovirus expressed aptamer sensitizes TNFalpha-induced apoptosis. *Biochem Biophys Res Commun* 2007; **359**: 475–480.
22 Yang ZF, Poon RT. Vascular changes in hepatocellular carcinoma. *Anat Rec (Hoboken)* 2008; **291**: 721–734.
23 Wu XZ, Xie GR, Chen D. Hypoxia and hepatocellular carcinoma: the therapeutic target for hepatocellular carcinoma. *J Gastroenterol Hepatol* 2007; **22**: 1178–1182.
24 Jain RK, Duda DG, Clark JW, Loeffler JS. Lessons from phase III clinical trials on anti-VEGF therapy for cancer. *Nat Clin Pract Oncol* 2006; **3**: 24–40.
25 Sitohy B, Nagy JA, Jaminet SC, Dvorak HF. Tumor surrogate blood vessel subtypes exhibit differential susceptibility to anti-VEGF therapy. *Cancer Res* 2011; **71**: 7021–7028.
26 Wang F, Xue X, Wei J, An Y, Yao J, Cai H *et al.* hsa-miR-520h downregulates ABCG2 in pancreatic cancer cells to inhibit migration, invasion, and side populations. *Br J Cancer* 2010; **103**: 567–574.
27 Eccles SA, Court W, Patterson L, Sanderson S. *In vitro* assays for endothelial cell functions related to angiogenesis: proliferation, motility, tubular differentiation, and proteolysis. *Method Mol Biol* 2009; **467**: 159–181.
28 Liu LZ, Fang J, Zhou Q, Hu X, Shi X, Jiang BH. Apigenin inhibits expression of vascular endothelial growth factor and angiogenesis in human lung cancer cells: implication of chemoprevention of lung cancer. *Mol Pharmacol* 2005; **68**: 635–643.
29 Weidner N. Current pathologic methods for measuring intratumoral microvessel density within breast carcinoma and other solid tumors. *Breast Cancer Res Treat* 1995; **36**: 169–180.

Supplementary Information accompanies the paper on the Oncogene website (http://www.nature.com/onc)

Downregulation of vasohibin-2, a novel angiogenesis regulator, suppresses tumor growth by inhibiting angiogenesis in endometrial cancer cells

TAKAHIRO KOYANAGI[1,2], YASUSHI SAGA[1], YOSHIFUMI TAKAHASHI[1,2], YASUHIRO SUZUKI[2], MITSUAKI SUZUKI[1] and YASUFUMI SATO[2]

[1]Department of Obstetrics and Gynecology, School of Medicine, Jichi Medical University, Shimotsuke-shi, Tochigi 329-0498; [2]Department of Vascular Biology, Institute of Development, Aging and Cancer, Tohoku University, Aoba-ward, Sendai 980-8575, Japan

Received October 10, 2012; Accepted December 31, 2012

DOI: 10.3892/ol.2013.1119

Abstract. The vasohibin-2 (VASH2) gene was originally found to be expressed in infiltrating mononuclear cells of a mouse model of hypoxia-induced subcutaneous angiogenesis. These cells are mobilized from bone marrow to promote angiogenesis. Recently, VASH2 has been demonstrated to be expressed in several types of cancer in which it promotes tumor development through angiogenesis. However, its role in endometrial cancer remains unknown. Using quantitative reverse transcription-polymerase chain reaction (RT-PCR), we found that VASH2 was overexpressed in several human endometrial cancer cell lines, including the HEC50B cell line, which we used to further examine the role of VASH2. Although knockdown of VASH2 with stable transfection of shRNA had little effect on the proliferation of HEC50B cells *in vitro*, knockdown in an *in vivo* murine xenograft model inhibited tumor growth by decreasing tumor angiogenesis. In addition, the supernatant from HEC50B cells that expressed VASH2 significantly promoted the proliferation of human umbilical vein endothelial cells. By contrast, knockdown of VASH2 significantly attenuated the proliferative effect. These results indicate that VASH2 contributes to the development of endometrial cancer by promoting angiogenesis through a paracrine mode of action. Consequently, VASH2 may be considered to be a novel molecular target for endometrial cancer therapy.

Introduction

Endometrial cancer is the most frequent gynecological malignancy and the fourth most common type of cancer in females in the United States (1). When endometrial cancer is localized to the uterus, it is often detected at an early stage; therefore, the overall survival rate is >80% (1). However, the prognosis of advanced endometrial cancer remains poor (2). Surgery, radiotherapy and multidrug chemotherapy have all been used to treat advanced endometrial cancer with little success. Therefore, limited improvements in overall treatment outcomes have been observed in endometrial cancer over the past 30 years (1). Therefore, novel strategies, such as anti-angiogenic therapy and targeted molecular therapy, may be useful in improving the prognosis of endometrial cancer.

Angiogenesis is a hallmark of malignant tumor development, and is important in the growth of primary, metastatic and disseminated lesions of endometrial cancer (3). Therefore, anti-angiogenic therapy may be effective in treating endometrial cancer. At present, anti-angiogenic therapy has been approved for several types of cancer, including colon, lung, breast and kidney cancer. Furthermore, several drugs that target vascular endothelial growth factor (VEGF) signals are already in clinical use (4). While the effectiveness of these drugs is encouraging, resistance to anti-angiogenic therapy has been demonstrated in several reviews (5-8). To overcome these problems, novel molecular targets for anti-angiogenic therapy need to be discovered.

The vasohibin family includes vasohibin-1 (VASH1) and vasohibin-2 (VASH2). In endothelial cells (ECs), VASH1 is selectively induced by angiogenesis stimulators, such as VEGF and basic fibroblast growth factor (bFGF). VASH1 functions as an intrinsic negative feedback regulator at the termination zone of angiogenesis (9). VASH2 is a homolog of VASH1, and the VASH2 gene is highly expressed in bone marrow-derived mononuclear cells and weakly expressed in ECs. In contrast to VASH1, VASH2 has been found to promote angiogenesis at the sprouting front in a mouse model of hypoxia-induced subcutaneous angiogenesis (10). To date, there are a limited number of studies available in the literature concerning the correlation between VASH2 and tumor angiogenesis (11,12). Recently, we demonstrated that VASH2 contributes to the development of tumor growth and peritoneal dissemination by promoting angiogenesis in human ovarian serous adenocarcinoma (12).

Correspondence to: Dr Yasushi Saga, Department of Obstetrics and Gynecology, School of Medicine, Jichi Medical University, 3311-1 Yakushiji, Shimotsuke-shi, Tochigi 329-0498, Japan
E-mail: saga@jichi.ac.jp

Key words: endometrial cancer, vasohibin-2, tumor angiogenesis, molecular-targeted therapy, endothelial cells

However, the specific role of VASH2 in endometrial cancer remains unknown.

In this study, we used a short hairpin RNA (shRNA) vector to silence VASH2 expression in a VASH2-expressing endometrial cancer cell line, to further elucidate the relationship between VASH2 expression and endometrial cancer progression. Moreover, we investigated the function of VASH2 in endometrial cancer angiogenesis to develop a VASH2-targeted anti-angiogenic molecular therapy for endometrial cancer.

Materials and methods

Cell culture. Human endometrial cancer cell lines, HEC1A and HEC50B, were obtained from the Japanese Collection of Research Bioresources (JCRB; Osaka, Japan), and were maintained as described previously (13,14). The Ishikawa cell line (clone 3H12) was a gift from Dr M. Nishida (Department of Obstetrics and Gynecology, National Hospital Organization, Kasumigaura Medical Center, Ibaraki, Japan), and was maintained as described previously (15). Cells were cultured in RPMI-1640 medium (Wako Pure Chemical Industries, Ltd., Osaka, Japan) supplemented with 10% heat-inactivated fetal bovine serum (FBS; BioWest S.A.S, Nuaillé, France). Human umbilical vein endothelial cells (HUVECs) were obtained from Kurabo Industries, Ltd. (Osaka, Japan) and were cultured in type I collagen-coated dishes (Iwaki, Chiba, Japan) in endothelial basal medium (EBM)-2 (Lonza, Walkersville, MD, USA) supplemented with EGM-2-MV-SingleQuots (Lonza) containing VEGF, bFGF, insulin-like growth factor-1, epidermal growth factor and 5% FBS. All cells were cultured at 37°C in a humidified atmosphere with 5% CO_2.

shRNA stable cell line and control cell line. The DNA oligonucleotide sequences encoding shRNA targeting VASH2 included forward: 5'-CACGGGGCAGATTATAAGAAT TACGTGTGCTGTCCGTAATTCTTGTAGTCTGCTCCTT TTT-3' and reverse: 5'-CCCCGTCTAATATTCTTAATG CACACGACAGGCATAAGAACATCAGACGAGGAAAAA TACG-3'. The oligonucleotides were synthesized, annealed and inserted into the *Bsp*MI site of the piGENE PURhU6 vector (16), which contained a human U6 promoter and a puromycin resistance gene. The shRNA expression plasmid (piGENE PURhU6/shVASH2) and control plasmid (piGENE PURhU6) were transfected into HEC50B cells by the use of Lipofectamine LTX and Plus Reagent (Invitrogen Life Technologies, Carlsbad, CA, USA) according to the manufacturer's instructions. Following transfection, the cells were selected in puromycin-containing medium (Calbiochem, La Jolla, CA, USA). Subsequently, VASH2-knockdown clones and control clones were established.

Reverse transcription-polymerase chain reaction (RT-PCR). Total RNA was extracted from cell cultures using Isogen (Nippon Gene, Toyama, Japan) according to the manufacturer's instructions. The concentration of extracted RNA was determined using the Nanodrop 2000c spectrophotometer (Thermo Scientific, Wilmington, DE, USA). First-strand cDNA was generated with ReverTra Ace (Toyobo Co., Ltd., Osaka, Japan). The RT-PCR procedure was performed in a DNA thermal cycler (Takara Bio, Inc., Tokyo, Japan). PCR conditions consisted of an initial denaturation step at 94°C for 5 min, followed by 35 cycles comprising a 15-sec phase at 94°C (denaturation), a 30-sec phase at 56°C (annealing) and a 30-sec phase at 72°C (extension). PCR products were separated on a 2% agarose gel and visualized under ultraviolet rays by ethidium bromide staining. The primer pairs used were as follows: forward, 5'-ACCACAGTCCATGCCATCAC-3' and reverse, 5'-TCCACCACCCTGTTGCTGTA-3' for human GAPDH gene; and forward, 5'-ACGTCTCAAAGATGCTGAGG-3' and reverse, 5'-CTCTCCGACCCAAGTGAGAA-3' for human VASH2.

Quantitative real-time RT-PCR. cDNA was synthesized as described previously. The specific primer for human VASH2 was the same as that for RT-PCR. The CFX96 real-time PCR detection system was used with the reagent SYBR Premix Ex Taq™ (Takara Bio, Inc.) for real-time PCR. PCR conditions included an initial denaturation step at 95°C for 3 min, followed by 50 cycles comprising a 10-sec phase at 95°C, a 10-sec phase at 56°C and a 30-sec phase at 72°C. Amplification of GAPDH was used as an endogenous control. Relative gene expression levels were calculated using the comparative Ct method.

Proliferation of tumor cells. Proliferation of tumor cells was measured by performing the TetraColor ONE cell proliferation assay (17). Briefly, cells were seeded at a density of $2x10^3$ cells/well in a 96-well plate and incubated at 37°C. After 24, 48, 72 and 96 h, 5 μl of TetraColor ONE (Seikagaku Co., Tokyo, Japan) was added to each well. The mixture was subsequently incubated for an additional 2 h and absorbance at 450 nm was monitored.

Proliferation of ECs. The VASH2-knockdown clones of HEC50B and HEC50B cells transfected with empty vector were cultured for 24 h. The conditioned medium (CM) was obtained from each culture. Subsequently, cellular components were removed from the CM using a Millex GP filter (0.22 μm; PES, 33MM; Millipore, Billerica, MA, USA). HUVECs were plated in a 96-well plate at a density of $2x10^3$ cells/well and cultured in medium containing the CM obtained previously. After 48 h, the proliferation of HUVECs was measured using the TetraColor ONE as previously described.

Mouse xenograft model of human endometrial cancer. Female 6- to 8-week old BALB/c nude mice were obtained from CLEA Japan, Inc. (Tokyo, Japan). The experimental protocols were approved and conducted according to the guidelines for animal experimentation of Jichi Medical University. Tumor cells were subcutaneously transplanted into the back of mice at a concentration of $4x10^6$ cells/mouse. The dimensions of the tumor were measured twice per week and the volume was calculated using the following formula: Volume=1/2x(long diameter)x(short diameter)^2. For the immunohistochemical analysis of tumor angiogenesis, the tumors were frozen in optimal cutting temperature (OCT) compound (Sakura, Tokyo, Japan), cut into 7-μm sections, fixed in methanol for 20 min at -20°C and blocked with 1% bovine serum albumin in phosphate-buffered saline (PBS) for 45 min at room temperature. Primary antibody reactions were performed overnight at 4°C with rat monoclonal

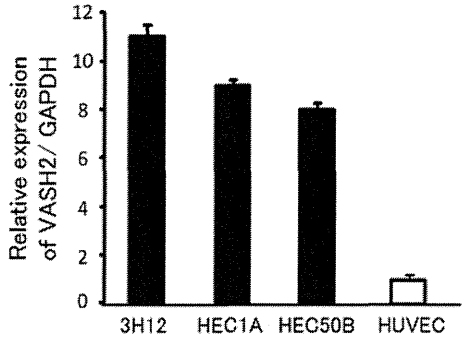

Figure 1. Expression of vasohibin-2 (VASH2) in human endometrial cancer cell lines. Quantitative reverse transcription-polymerase chain reaction (RT-PCR) shows the expression of VASH2 in various cell lines of endometrial cancer. VASH2 expression in human umbilical vein endothelial cells (HUVECs) is defined as 1. Means and standard deviations are shown (n=3).

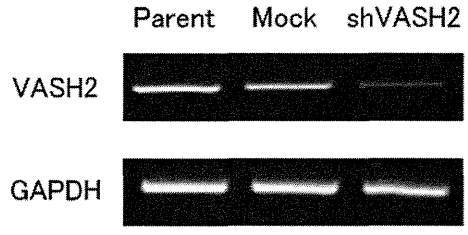

Figure 2. Establishment of vasohibin-2 (VASH2) knockdown clone in the HEC50B cell line. VASH2 knockdown (shVASH2) clones from HEC50B cells and their control mock transfectant were established. Reverse transcription-polymerase chain reaction (RT-PCR) shows the knockdown of VASH2 in shVASH2 clones established from HEC50B cells.

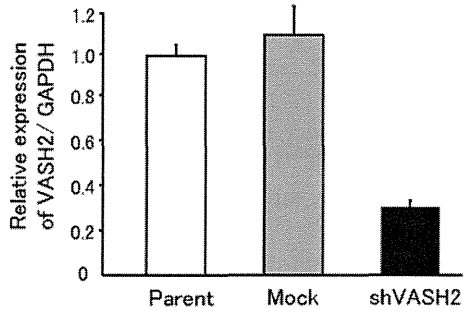

Figure 3. Gene expression of vasohibin-2 (VASH2) in HEC50B transfectants. Quantitative reverse transcription-polymerase chain reaction (RT-PCR) shows the knockdown of VASH2 in VASH2-knockdown (shVASH2) clones with a knockdown efficacy >70%. VASH2 expression in the parent cell line is defined as 1. Means and standard deviations are shown (n=5).

antibody against mouse CD31 (BD Biosciences, San Diego, CA, USA) at a dilution of 1:500. Secondary antibody reactions were performed for 1 h at room temperature with Alexa Fluor 488-conjugated donkey anti-rat IgG (Molecular Probes, Eugene, OR, USA) at a dilution of 1:500. After washing 3 times with PBS, the sections were covered with fluorescent mounting medium (Dako, Carpintera, CA, USA). All samples were analyzed with a BZ-9000 fluorescence microscope (Keyence, Osaka, Japan) at room temperature. To evaluate tumor angiogenesis, the vascular luminal area was calculated using five different fields of each tumor section with BZ-H1C software (Keyence).

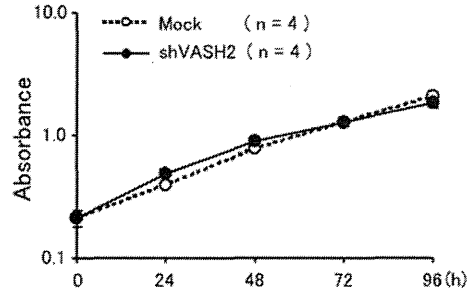

Figure 4. *In vitro* proliferation of HEC50B transfectants. The proliferation of vasohibin-2-knockdown (shVASH2) clones and of their control mock transfectants were compared under the same cell culture conditions *in vitro*. Knockdown of VASH2 did not affect the *in vitro* proliferation of HEC50B. Means and standard deviations are shown (n=4).

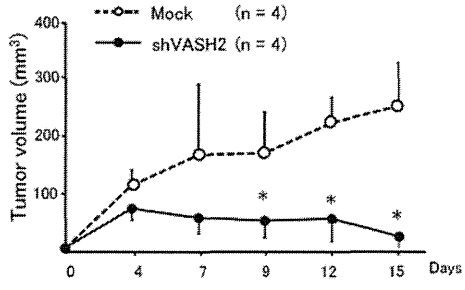

Figure 5. Subcutaneous xenograft model of HEC50B transfectants. Mock or vasohibin-2-knockdown (shVASH2) clones established from HEC50B cells were inoculated subcutaneously into nude mice, and the serial tumor growth was compared in terms of tumor volume. Knockdown of VASH2 significantly inhibited the subcutaneous tumor growth *in vivo*. Means and standard deviations are shown (n=4). *P<0.05 vs. mock transfectants.

Statistical analysis. A Student's t-test was used to test for a significant difference between the 2 groups. P<0.05 was considered to indicate a statistically significant difference.

Results

VASH2 expression. To examine the possible involvement of VASH2 in endometrial cancer, we analyzed human endometrial cancer cell lines by quantitative RT-PCR. As demonstrated in Fig. 1, VASH2 mRNA expression was considerably higher in several human endometrial cancer cell lines than in the HUVECs.

Knockdown of VASH2 and its effects in vitro and in vivo. To clarify the function of VASH2 in endometrial cancer, we performed a loss-of-function experiment by knocking down VASH2 expression. We used HEC50B, an endometrial cancer cell line with high VASH2 expression, for the following experiments. By the transfection of shRNA, we established the VASH2-knockdown (shVASH2) clone from HEC50B (Fig. 2). The efficacy of knockdown was >70% (Fig. 3). Knockdown of VASH2 did not affect the *in vitro* proliferation of HEC50B cells (Fig. 4). We then inoculated the shVASH2 clone subcutaneously into nude mice, and observed a significant inhibition of tumor growth in the shVASH2 group compared with the control mock group (Fig. 5). Furthermore, we analyzed angiogenesis in the tumors of the mouse xenograft model. As

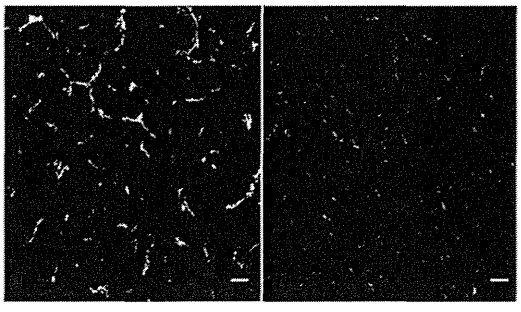

Figure 6. Immunofluorescent staining of CD31 to show tumor angiogenesis. Frozen sections of tumors obtained from mock or HEC50B shVASH2 clones were immunostained with anti-CD31 antibody. Scale bar, 50 μm.

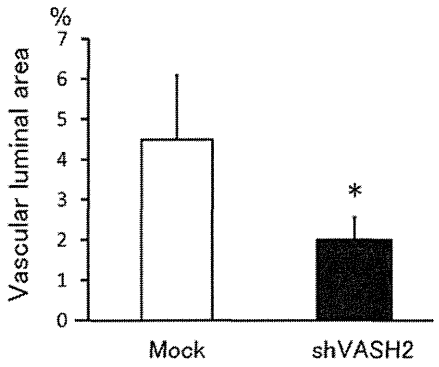

Figure 7. Quantification of tumor angiogenesis. The vascular luminal area was calculated from five different fields of each tumor section and then compared. Tumor angiogenesis decreased significantly in tumors derived from vasohibin-2-knockdown (shVASH2) clones. Means and standard deviations are shown (n=4). *P<0.05 vs. mock.

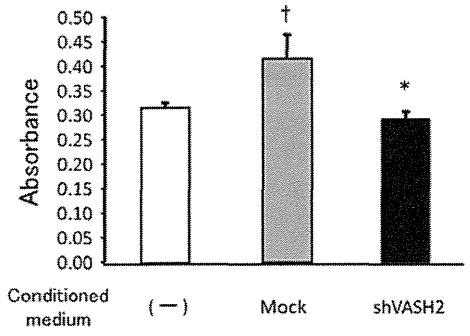

Figure 8. Effect of secreted vasohibin-2 (VASH2) on endothelial cell (EC) proliferation. The proliferation of human umbilical vein endothelial cells (HUVECs) incubated without conditioned medium (CM) or with CM from VASH2-knockdown (shVASH2) clones or mock transfectants of HEC50B cells was compared *in vitro*. Secreted VASH2 promoted the proliferation of HUVECs and knockdown of VASH2 attenuated that effect. Means and standard deviations are shown (n=4). †P<0.05 vs. without CM. *P<0.05 vs. with CM from mock transfectants.

expected, tumor angiogenesis was significantly inhibited in the shVASH2 tumors, as assessed by immunofluorescent staining of CD31 (Figs. 6 and 7).

Effect of secreted VASH2 on EC proliferation. Members of the vasohibin family are secretory proteins that bind to the intracellular small vasohibin-binding protein (SVBP) (18). To investigate the effect of VASH2 on the ECs, we evaluated the proliferation of HUVECs by using the CM from shVASH2 clones or from mock transfectants of HEC50B. As demonstrated in Fig. 8, secreted VASH2 significantly promoted the proliferation of HUVECs, whereas knockdown of VASH2 significantly attenuated the proliferative effect.

Discussion

In the present study, we examined the correlation between VASH2 and endometrial cancer cell for the first time. VASH2 was expressed in human endometrial cancer cell lines, and the specific knockdown of VASH2 from the endometrial cancer cell line, HEC50B, significantly inhibited tumor growth by decreasing tumor angiogenesis. In addition, the experiment using the CM revealed that secreted VASH2 significantly promoted the proliferation of HUVECs. These results suggest that VASH2 secreted from the cancer cells acts on neighboring ECs to stimulate angiogenesis in a paracrine manner, and thus contributes to the development of endometrial cancer.

Angiogenesis is recognized as a principal hallmark of various types of cancer (19). There are a number of angiogenic stimulators, one of the most important of which is VEGF, which stimulates EC migration and proliferation, as well as EC tube formation. VEGF is the prototype of the VEGF family, and its pro-angiogenic signals are mainly transmitted via its type 2 receptor (VEGFR2) on ECs (20). In endometrial cancer tissues, VEGF expression is associated with elevated tumor vascularization as measured by microvessel density (3), and is a predictive marker for decreased 5-year survival in patients with advanced endometrial carcinoma (21-23). Thus, anti-angiogenic therapy is considered to be a promising option for treating endometrial cancer. Current VEGF-targeted therapeutic drugs, including bevacizumab (a monoclonal antibody against VEGF-A), have yielded promising results in animal models and clinical trials of endometrial cancer (3,24). However, resistance to such therapeutics may occur, owing to the development of compensatory mechanisms for producing angiogenic factors other than VEGF, or the recruitment of bone marrow-derived angiogenic cells. Therefore, alternative targets for anti-angiogenic therapy, a number of which are being investigated, ought to be sought (25). Taking its stimulatory effect on angiogenesis into account, VASH2 may be a novel molecular target for the treatment of endometrial cancer.

While the putative VASH2 receptor and its downstream signaling are currently under investigation, a number of studies have examined the novel function of VASH2. In one study, an autocrine and paracrine mode of action for VASH2 was found to enhance the expression of FGF-2 and VEGF by nuclear factor-κB upregulation in hepatocellular carcinoma (HCC) cells (11). Furthermore, VASH2 has been found not only to accelerate angiogenesis but also to promote HCC cell proliferation (11). In ovarian serous adenocarcinoma cells, the expression of VASH2 was inversely correlated with that of miR-200b, which represses the expression of ZEB1 and ZEB2, the products of which are key to epithelial-to-mesenchymal transition (26). Therefore, VASH2 may possess other tumor-promoting functions, such as invasion and migration. These features of VASH2 require further investigation.

The local balance between angiogenesis stimulators and inhibitors, both of which are activated simultaneously during angiogenesis, determines the occurrence and progression of angiogenesis. In contrast to VEGF and VASH2, VASH1 has been shown to both inhibit EC angiogenesis and protect EC from apoptosis (11). As a VEGF-independent and EC-extrinsic angiogenesis regulator, VASH2 is considered to be a novel target for anti-angiogenic therapy that enables the toxic side effects of anti-VEGF therapy, such as hypertension and proteinuria, to be avoided. Moreover, the twin combination of VASH2 inhibition and VASH1 upregulation would be a powerful anti-cancer strategy.

In summary, VASH2 contributes to the development of endometrial cancer by regulating angiogenesis through paracrine effects. As such, it constitutes a promising molecular target for endometrial cancer therapy.

Acknowledgements

This study was supported by The Research Award to JMU Graduate Students (T.K. and Y.T.).

References

1. Jemal A, Siegel R, Xu J and Ward E: Cancer Statistics, 2010. CA Cancer J Clin 60: 277-300, 2010.
2. Wolfson AH, Sightler SE and Markoe AM: The prognostic significance of surgical staging for carcinoma of the endometrium. Gynecol Oncol 45: 142-146, 1992.
3. Kamat AA, Merritt WM, Coffey D, *et al*: Clinical and biological significance of vascular endothelial growth factor in endometrial cancer. Clin Cancer Res 13: 7487-7495, 2007.
4. Kowanetz M and Ferrara N: Vascular endothelial growth factor signaling pathways: therapeutic perspective. Clin Cancer Res 12: 5018-5022, 2006.
5. Ortega J, Vigil CE and Chodkiewicz C: Current progress in targeted therapy for colorectal cancer. Cancer Control 17: 7-15, 2010.
6. Koutras AK, Fountzilas G, Makatsoris T, Peroukides S and Kalofonos HP: Bevacizumab in the treatment of breast cancer. Cancer Treat Rev 36: 75-82, 2010.
7. Tamaskar I and Pili R: Update on novel agents in renal cell carcinoma. Expert Rev Anticancer Ther 9: 1817-1827, 2009.
8. Norden AD, Drappatz J and Wen PY: Antiangiogenic therapies for high-grade glioma. Nat Rev Neurol 5: 610-620, 2009.
9. Watanabe K, Hasegawa Y, Yamashita H, *et al*: Vasohibin as an endothelium-derived negative feedback regulator of angiogenesis. J Clin Invest 114: 898-907, 2004.
10. Kimura H, Miyashita H, Suzuki Y, *et al*: Distinctive localization and opposed roles of vasohibin-1 and vasohibin-2 in the regulation of angiogenesis. Blood 113: 4810-4818, 2009.
11. Xue X, Gao W, Sun B, *et al*: Vasohibin 2 is transcriptionally activated and promotes angiogenesis in hepatocellular carcinoma. Oncogene: May 21, 2012 (Epub ahead of print).
12. Takahashi Y, Koyanagi T, Suzuki Y, *et al*: Vasohibin-2 expressed in human serous ovarian adenocarcinoma accelerates tumor growth by promoting angiogenesis. Mol Cancer Res: Jul 23, 2012 (Epub ahead of print).
13. Kuramoto H, Tamura S and Notake Y: Establishment of a cell line of human endometrial adenocarcinoma in vitro. Am J Obstet Gynecol 114: 1012-1019, 1972.
14. Suzuki M, Kuramoto H, Hamano M, Shirane H and Watanabe K: Effects of oestradiol and progesterone on the alkaline phosphatase activity of a human endometrial cancer cell-line. Acta Endocrinol (Copenh) 93: 108-113, 1980.
15. Nishida M: The Ishikawa cells from birth to the present. Hum Cell 15: 104-117, 2002.
16. Miyagishi M and Taira K: Strategies for generation of an siRNA expression library directed against the human genome. Oligonucleotides 13: 325-333, 2003.
17. Yamamoto O, Hamada T, Tokui N and Sasaguri Y: Comparison of three in vitro assay systems used for assessing cytotoxic effect of heavy metals on cultured human keratinocytes. J UOEH 23: 35-44, 2001.
18. Suzuki Y, Kobayashi M, Miyashita H, Ohta H, Sonoda H and Sato Y: Isolation of a small vasohibin-binding protein (SVBP) and its role in vasohibin secretion. J Cell Sci 123: 3094-3101, 2010.
19. Hanahan D and Weinberg RA: The hallmarks of cancer. Cell 100: 57-70, 2000.
20. Ferrara N: Vascular endothelial growth factor. Arterioscler Thromb Vasc Biol 29: 789-791, 2009.
21. McMeekin DS, Sill MW, Benbrook D, *et al*; Gynecologic Oncology Group: A phase II trial of thalidomide in patients with refractory endometrial cancer and correlation with angiogenesis biomarkers: a Gynecologic Oncology Group study. Gynecol Oncol 105: 508-516, 2007.
22. Sanseverino F, Santopietro R, Torricelli M, *et al*: pRb2/p130 and VEGF expression in endometrial carcinoma in relation to angiogenesis and histopathologic tumor grade. Cancer Biol Ther 5: 84-88, 2006.
23. Hirai M, Nakagawara A, Oosaki T, Hayashi Y, Hirono M and Yoshihara T: Expression of vascular endothelial growth factors (VEGF-A/VEGF-1 and VEGF-C/VEGF-2) in postmenopausal uterine endometrial carcinoma. Gynecol Oncol 80: 181-188, 2001.
24. Cerezo L, Cardenes H and Michael H: Molecular alterations in the pathogenesis of endometrial adenocarcinoma. Therapeutic implications. Clin Transl Oncol 8: 231-241, 2006.
25. Saranadasa M and Wang ES: Vascular endothelial growth factor inhibition: conflicting roles in tumor growth. Cytokine 53: 115-129, 2011.
26. Korpal M and Kang Y: The emerging role of miR-200 family of microRNAs in epithelial-mesenchymal transition and cancer metastasis. RNA Biol 5: 115-119, 2008.

ARTICLE IN PRESS

Human Pathology (2013) xx, xxx–xxx

Human PATHOLOGY

www.elsevier.com/locate/humpath

Original contribution

Proliferation and maturation of intratumoral blood vessels in non–small cell lung cancer☆,☆☆

Samaneh Yazdani[a], Yasuhiro Miki PhD[a], Kentaro Tamaki MD, PhD[b,c], Katsuhiko Ono CT[a], Erina Iwabuchi[a], Keiko Abe MD, PhD[a], Takashi Suzuki MD, PhD[a], Yasufumi Sato MD, PhD[d], Takashi Kondo MD, PhD[e], Hironobu Sasano MD, PhD[a,c,*]

[a]*Department of Pathology, Tohoku University Graduate School of Medicine, Sendai, 980-8575, Japan*
[b]*Department of Surgical Oncology, Tohoku University Graduate School of Medicine, Sendai, 980-8575, Japan*
[c]*Department of Pathology, Tohoku University Hospital, Sendai, 980-8574, Japan*
[d]*Department of Vascular Biology, Institute of Development, Aging and Cancer, Tohoku University, Sendai, 980-8575, Japan*
[e]*Department of Thoracic Surgery, Institute of Development, Aging and Cancer, Tohoku University, Sendai, 980-8575, Japan*

Received 19 October 2012; revised 8 January 2013; accepted 9 January 2013

Keywords:
Immunohistochemistry;
Lung;
Angiogenesis;
Pericyte;
Vasohibin-1

Summary Non–small cell lung carcinoma is one of the most common leading causes of cancer mortality, and studying the features of intratumoral vessels, especially their generation and maturation, has become more important because of the recent application of antiangiogenic therapy. Vasohibin-1 has been recently considered one of the immunohistochemical markers for identifying neovascularization in archival materials. In addition, the functional maturation of blood vessels is considered to be related to pericyte formation around endothelial cells. Therefore, in this study, we evaluated the status of angiogenesis and maturation of intratumoral blood vessels in 93 patients with non–small cell lung carcinoma (50 with adenocarcinoma and 43 with squamous cell carcinoma) using immunohistochemistry of vasohibin-1, endoglin, CD31, and nestin. The vasohibin-1/CD31-positive ratio was significantly ($P = .03$) correlated with the Ki-67/CD31 ratio, confirming that the vasohibin-1/CD31-positive ratio represented the status of neovascularization in lung cancer. There were no statistically significant differences in vasohibin-1/CD31 ratios between adenocarcinoma and squamous cell carcinoma in both inner ($P = .39$) and outer areas ($P = .36$) of the tumor. The vasohibin-1/nestin-positive ratio, which represents the degrees of vascular maturation in proliferative vessels, was significantly lower in inner areas of adenocarcinoma (0.4 ± 0.1) than those in squamous cell carcinoma (0.8 ± 0.1) ($P = .02$). These results demonstrated that the degrees of maturation in newly formed blood vessels were less developed in inner areas of squamous cell carcinoma than adenocarcinoma, which may account partly for the complications of antivascular endothelial growth factor therapy more frequently detected in patients with squamous cell carcinoma.

1. Introduction

Lung cancer is the most common cause of cancer mortality in the world [1]. Non–small cell lung cancer (NSCLC) accounts for nearly 80% of all lung cancer cases [1]. NSCLC is histologically composed of adenocarcinoma (ADC),

☆ Disclosure statement: There are no conflicts of interests in any of the authors.

☆☆ This work is partly supported by Grant-in-Aid for Scientific Research from the Japanese Ministry of Education, Culture, Sports, Science and Technology.

* Corresponding author. Department of Pathology, Tohoku University School of Medicine, 2-1 Seiryou-machi, Aoba-ku, Sendai, Japan.
E-mail address: hsasano@patholo2.med.tohoku.ac.jp (H. Sasano).

0046-8177/$ – see front matter © 2013 Elsevier Inc. All rights reserved.
http://dx.doi.org/10.1016/j.humpath.2013.01.004

squamous cell carcinoma (SCC), and other subtypes [2]. Most lung cancer cases are still detected at relatively advanced clinical stages, and systemic therapy plays pivotal roles in improving the overall survival of these patients [3]. The antiangiogenic agents have been administered in patients with NSCLC [3], including vascular endothelial growth factor (VEGF) receptor–targeted agents, which are considered to ultimately inhibit tumor cell proliferation through the suppression of new vessel formation [4]. Among these anti-VEGF agents, bevacizumab is a recombinant humanized murine monoclonal antibody [5] and selectively binds to VEGF and blocks its binding to the receptor [6]. Bevacizumab has demonstrated clinical efficacy even as a first-line treatment for patients with NSCLC [7]. However, fatal intratumoral hemorrhage has been reported in up to 30% of the patients with SCC during the course of bevacizumab therapy, and bevacizumab is therefore currently administered only to those with histologically confirmed ADC [7].

Therefore, it has become pivotal to evaluate the status of intratumoral vasculature in NSCLC and to subsequently compare them between ADC and SCC. Microvessel density (MVD) examined by CD34 in ADC was reported to be higher than that in SCC [8], but the status of neovascularization and vascular maturation has not been examined in NSCLC, to the best of our knowledge. Tamaki et al [9,10] recently reported that the ratio of vasohibin-1 (VASH-1), an endothelium-originated negative feedback regulator of angiogenesis, among CD31-positive vessels did represent the status of angiogenesis [9,10]. Tamaki et al [9,10] also subsequently demonstrated that the ratio of positive Ki-67 endothelial cells was significantly correlated with the VASH-1/CD31-positive ratio in these breast cancer cases, confirming that the VASH-1/CD31-positive ratio represented the degrees of angiogenesis. In addition, endoglin, a transmembrane protein also known as CD105, was proposed as an effective immunohistochemical marker of neovascularization in various human neoplasms [11].

In a mature blood vessel, endothelium, which forms the inner lining of vessel wall, is encircled by pericytes [12]. In tumor tissues, pericytes were frequently detected but also reported to be loosely attached to the endothelium and their cytoplasm spread away from the vascular wall compared with those in nonneoplastic tissues [13]. These differences of vascular structures in previously mentioned cancer tissues are currently considered to cause the fragility of vascular wall and, eventually, increase the risks of hemorrhage [13,14]. Pericytes have been immunohistochemically identified in surgical pathology materials using several markers such as smooth muscle actin (α-SMA), desmin, nestin, and sulfatide or high-molecular-weight melanoma-associated antigen (NG-2) [15].

Therefore, we first immunolocalized VASH-1, endoglin, and CD31 to evaluate the status of neovascularization in ADC and SCC in both inner and outer areas of the tumor as well as extratumoral areas because of the reported differences in the biological features of intratumoral vessels between inner and outer areas of NSCLC [16,17]. We then correlated the VASH-1/CD31 and endoglin/CD31 with Ki-67/CD31-positive ratios to validate the significance of these markers in identifying the proliferating vessels in surgical pathology materials of NSCLC. We subsequently immunolocalized α-SMA, desmin, nestin, and NG-2, the previously reported markers of pericytes in ADC and SCC, and compared the results with those in histologically nonpathologic or normal lung tissues to study the status of vascular maturation in NSCLC. We finally compared CD31/nestin, VASH-1/nestin, and endoglin/nestin ratios between ADC and SCC to further explore the correlation between angiogenesis and maturation of vessels in these tumors.

2. Materials and methods

2.1. Patients

A total of 93 Japanese patients with NSCLC (50 with ADC and 43 with SCC) who had undergone surgical resection from 1993 to 1995 at Tohoku University Hospital, Sendai, Japan, were examined in this study. In addition, 10 histologically normal or nonpathologic lung cases were retrieved from the pathology file of the Tohoku University School of Medicine as control specimens. The average age of the patients was 65.4 years (23-81 years), and the relevant clinicopathologic findings are summarized in Table 1. The average age of the control patients examined in this study was 61.6 years (47-74 years), with 6 being male and 4 being female.

The research protocol of this study was approved by the Ethics Committee at the Tohoku University School of Medicine (No. 2010-571). None of these patients examined had received any forms of antineoplastic therapy before surgery.

2.2. Immunohistochemistry

In this study, we used 10% formalin-fixed and paraffin-embedded tissues. The slides were pretreated using an autoclave (120°C, 5 minutes), in citrate buffer (2 mmol/L citric acid and 9 mmol/L trisodium citrate dehydrate, pH 6.0) for nestin, NG-2, and CD31, in 10 nmol ethylenediaminetetraacetate (pH 8) for VASH-1, trypsin incubation (0.1 %) for 30 minutes at 37°C incubator for α-SMA as an antigen retrieval, and no antigen retrieval used for endoglin and desmin. The slides were then incubated with the primary antibodies overnight at 4°C. The primary antibodies for α-SMA, desmin, NG-2, VASH-1, endoglin, and CD31 were mouse monoclonal, and a rabbit polyclonal antibody was used for nestin. The concentration of the primary antibodies used was as follows: α-SMA (Dako Cytomation, Glostrup, Denmark; 1:300), desmin (Dako; 1:100), NG-2 (Millipore, USA; 1:400), nestin (Chemicon, Bilerica, MA, USA; 1:8000), VASH-1 (kindly provided by Prof Sato Y, Tohoku University, Tohoku, Japan; 1:400), endoglin (Dako; 1:100), and CD31 (Dako; 1:100).

The sections were then incubated with biotin-conjugated rabbit antimouse antibody or goat antirabbit antibody (Nichirei Biosciense, Tokyo, Japan), and the reactive sections

Table 1 Summary of clinicopathologic findings of the cases examined

Clinicopathologic variables	All categories	ADC (n = 50)	SCC (n = 43)
Sex	Male	32 (64%)	42 (98%)
	Female	18 (36%)	1 (2%)
Age (y) [a]	All	65 (35-78)	66 (23-81)
	Male	66 (37-78)	66 (23-81)
	Female	62 (35-78)	67
Stage [b]	I	26 (66%)	22 (55%)
	II	3 (7%)	6 (15%)
	III	11 (25%)	11 (27%)
	IV	1 (2%)	1 (3%)
Differentiation [c]	Well	18 (38%)	6 (14%)
	Moderate	23 (48%)	19 (44%)
	Poor	7 (14%)	18 (42%)
pT [d]	pT1	24 (56%)	11 (27%)
	pT2	16 (37%)	24 (59%)
	pT3	2 (5%)	1 (2%)
	pT4	1 (2%)	5 (12%)
pN [e]	pN0	38 (76%)	25 (61%)
	pN1	4 (8%)	8 (20%)
	pN2	8 (16%)	7 (17%)
	pN3	0 (0%)	1 (2%)
pM	pM0	49 (98%)	42 (98%)
	pM1	1 (2%)	1 (2%)
Survival time	Alive	28 (56%)	21 (49%)
	Dead	22 (44%)	22 (51%)

[a] Data are continuous variables, and the median with minimum-maximum values are presented.
[b] Information on tumor stages was available in 41 cases of ADC and 40 cases of SCC in our study.
[c] Information on differentiation was available in 48 cases of ADC in our investigation.
[d] Information on pT was available in 43 cases of ADC and 41 cases of SCC in our study
[e] Information on pN was available in 41 cases of SCC in our study.

were visualized using 3,3′-diaminobenzidine-tetracholoride and counterstained with hematoxylin.

2.3. Double immunostaining

Double immunohistochemistry of VASH-1/nestin and CD31/nestin was performed in all the cases examined, and Ki-67/CD31 was performed in a total of 30 cases (15 ADCs and 15 SCCs). Antigen retrieval was performed using an autoclave, in a citrate buffer for Ki-67 or MIB-1 antibody. The sections were incubated using Ki-67 mouse monoclonal primary antibody at the dilution of 1:100 after blocking the slides with normal rabbit serum. The sections were then immunostained as described earlier. 3,3′-Diaminobenzidine-tetracholoride was used as a colorimetric action of the first antibody, and alkaline phosphatase–conjugated avidin (Nichirei Biosciense, Tokyo, Japan) and alkaline phosphatase substrate kit (vector blue; Vector Laboratories, Burlingame, CA) were used for colorimetric reaction of the second antibody.

2.4. Evaluation of immunoreactivity and necrosis

MVD was assessed in both inner and outer areas of the tumor. An inner area corresponded to the central half, and the outer area referred to the peripheral half of the tumor diameter adjusted to the form of tumor, respectively [18,19]. *Extratumoral areas* were defined as the lung parenchymal tissues around the tumors in this study [20]. Results of immunoreactivity were independently evaluated by 2 of the authors (S.Y. and H.S.). Ten hot spots in inner and outer areas of the tumor as well as in extratumoral areas above and control cases were identified, which corresponded to those with high density of vessels in the tissues examined. The vessels were identified based on the lumen surrounded by endothelial cells or pericytes identified by immunohistochemistry. The hot spots were first selected by reviewing at low magnification (×40 and ×100), and the number of vessels was subsequently counted at higher power (×200). Clusters of endothelial cells that were continuously present because of various shapes of the vessel with different angles were tentatively interpreted as a single vessel in our present study [9].

The vessels that were covered in more than 50% of their circumference by pericyte marker–positive cells were tentatively defined as a single positive vessel for pericytes in our present study [13]. The neovascularization of blood vessels in the particular field was quantified by the ratio of VASH-1–positive vessels divided by CD31-positive vessels counted at the same areas and by the number of endothelial cells with Ki-67–positive nuclei divided by the total number of positive CD31 vessels [9].

Intratumoral necrosis was histologically graded as scores of 1 to 4, with necrosis scores of 1 indicating no necrotic areas; 2, necrotic areas of less than or equal to one-third; 3, necrotic area more than one-third to two-thirds; and 4, necrotic area more than two-thirds of the maximum width of the tumor [21].

2.5. Statistical analysis

The Student *t* test, Fisher exact test, and Wilcoxon rank sum test were performed for the analysis of the ratio of VASH-1 and CD31 using JMP software version Pro 9.0.2 (SAS Institute, Cary, NC). The correlation between VASH-1/CD31-positive and Ki-67/CD31 ratios was defined using Pearson correlation analysis. Multivariate analysis was performed by a proportional hazard analysis. The statistical significance was considered as a P value less than .05 in this study.

3. Results

3.1. Immunolocalization of endothelial cell markers in vessels of NSCLC

VASH-1, endoglin, and CD31 were detected only in histologically identified endothelial cells in NSCLC tissues

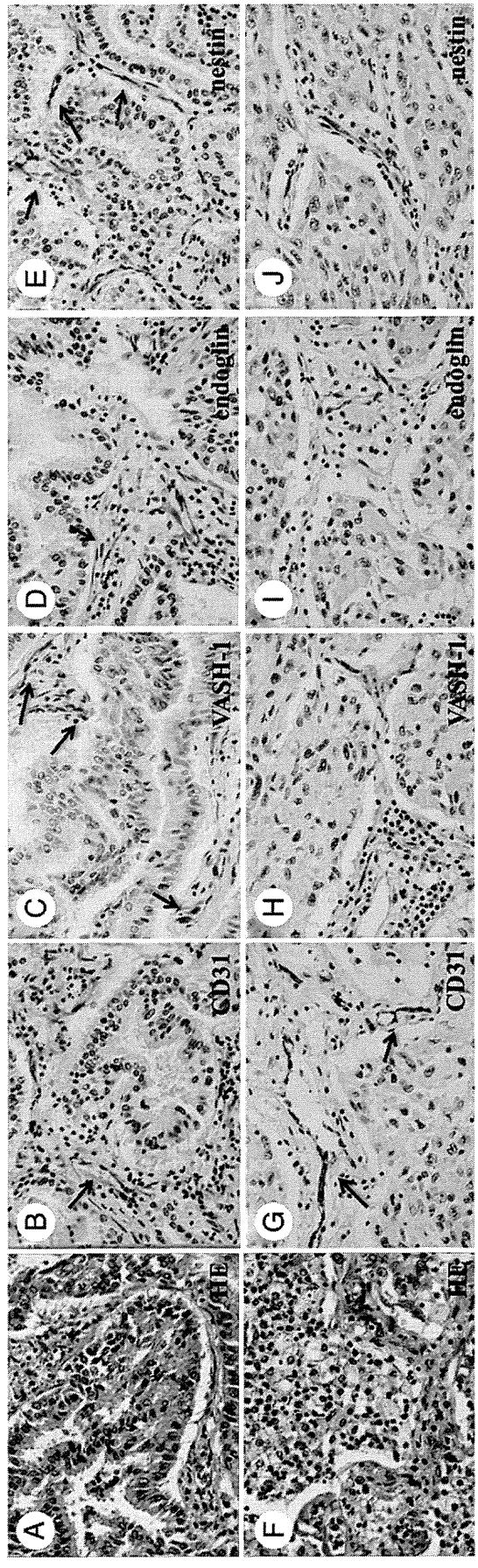

Fig. 1 Representative illustrations of histologic and immunohistochemical findings in NSCLC in the inner area. A-E, Staining of HE (A), CD31 (B), VASH-1 (C), endoglin (D), and nestin (E) in ADC. F-J, Staining of hematoxylin and eosin (F), CD31 (G), VASH-1 (H), endoglin (I), and nestin (J) in SCC. Arrows show positively stained vessels for each marker. Nestin expression in some vessels covered less than 50% of the vessel (×200).

examined (Fig. 1). The average number of these positive vessels for each marker in control cases, ADC, and SCC is summarized in Table 2. CD31-positive vessels in ADC was significantly higher in inner ($P < .001$) and outer areas ($P < .001$) than extratumoral area in the tissue specimens examined, but no significant differences between inner and outer areas were found ($P = .7$). CD31-positive vessels in SCC were also higher in both inner ($P = .07$) and outer areas ($P = .02$) than in extratumoral areas and significantly higher in outer than inner areas of SCC ($P = .01$). MVD or the number of CD31-positive vessels in the inner area of the tumor was significantly higher in ADC than in SCC ($P = .002$; Fig. 2A). The average number of VASH-1–positive microvessels as a cytoplasmic staining per each field (×200) in ADC was significantly higher in both inner ($P < .001$) and outer areas ($P < .001$) than in extratumoral areas and also significantly higher in outer than inner areas in ADC ($P = .01$). The average number of VASH-1–positive microvessels per each field in SCC was significantly higher in inner ($P = .01$) and outer areas ($P = .006$) than extratumoral areas, but no significant differences between inner and outer areas were found ($P = .07$). The number of positive VASH-1 vessels in both inner and outer areas of the tumors was significantly higher in ADC than in SCC ($P = .03$ and $P = .02$, respectively; Fig. 2B). The average number of endoglin-positive vessels did not show any significant differences between ADC and SCC ($P = .72$ and $P = .68$; Fig. 2C).

The ratio of VASH-1– to CD31-positive vessels in the same areas [9] of ADC was significantly higher in both inner ($P < .001$) and outer areas ($P < .001$) than in extratumoral areas, but there was no difference between inner and outer areas ($P = .45$). In SCC, the ratio was significantly higher in inner ($P = .006$) than in extratumoral areas, but there were no significant differences between inner and outer areas ($P = .32$). The VASH-1/CD31-positive ratio in inner and outer areas did not show any significant differences between ADC and SCC ($P = .39$ and $P = .36$, respectively; Fig. 2E). There were no significant differences of endoglin/CD31-positive ratios between ADC and SCC ($P = .33$ and $P = .61$, respectively; Fig. 2F).

3.2. Correlation between the ratios of VASH-1 or endoglin/CD31-positive vessels with Ki-67 labeling in endothelial cells

Statistically significant correlation was detected between the ratio of Ki-67/CD31- and VASH-1/CD31-positive vessels in the cases examined ($P = .03$; Figs. 3A and 4A, B), whereas no significant differences were detected between the ratio of Ki-67/CD31 and endoglin/CD31 ($P = .17$; Fig. 3B). VASH-1/CD31 tended to be correlated with endoglin/CD31, but the correlation did not reach statistical significance ($P = .08$; Fig. 3C).

3.3. The status of pericytes and their coverage identified by nestin immunohistochemistry in the intratumoral vessels of NSCLC

Nestin immunoreactivity was demonstrated to be most consistent with histologically identifiable pericytes in this study (data not shown). Therefore, we used nestin as an immunohistochemical marker of pericytes in the following studies.

The mean of pericytes counted based on nestin immunoreactivity as a cytoplasmic staining (Fig. 1E, J) did not show any significant differences between inner and extratumoral areas ($P = .45$), whereas it was significantly higher in outer than in extratumoral areas ($P = .004$) of ADC cases. In SCC, the value was significantly higher in outer than in inner areas of the tumor ($P = .01$). Overall nestin immunoreactivity in ADC in inner and outer areas was significantly higher than that in SCC ($P = .004$ and $P = .02$; Fig. 2D).

3.4. CD31/nestin and VASH-1/nestin ratios evaluated by double immunohistochemistry in the vessels of NSCLC

The ratio of CD31/nestin was subsequently obtained in individual cases of NSCLC. The CD31/nestin-positive ratio in ADC was significantly higher in inner ($P = .008$) and outer areas of the tumors ($P > .001$) than in extratumoral area, but

Table 2 Mean expression of examined markers in control, ADC cases, and SCC cases

Marker	Mean expression of MVD						
	Control	ADC			SCC		
		Inner area	Outer area	Extratumoral area	Inner area	Outer area	Extratumoral area
CD31	11.12 ± 7.41	15.11 ± 1.15	16.54 ± 1.48	8.12 ± 1.33	9.63 ± 1.34	13.20 ± 1.52	7.03 ± 1.67
VASH-1	4.62 ± 4.65	7.19 ± 0.61	10.14 ± 0.94	3.05 ± 0.69	5.38 ± 0.75	7.06 ± 1.03	2.97 ± 0.72
VASH-1/CD31-positive ratio	0.31 ± 0.20	0.84 ± 0.26	1.00 ± 0.21	0.32 ± 0.16	1.02 ± 0.20	0.91 ± 0.24	0.56 ± 0.18
Nestin	3.62 ± 2.31	15.37 ± 1.28	19.73 ± 1.85	13.65 ± 1.82	9.89 ± 1.43	13.44 ± 2.06	12.58 ± 2.29
CD31/Nestin-positive ratio	0.75 ± 0.21	1.59 ± 0.31	1.39 ± 0.22	0.84 ± 0.15	1.68 ± 0.34	1.21 ± 0.24	0.65 ± 0.27
VASH-1/Nestin-positive ratio	0.25 ± 0.05	0.42 ± 0.13	0.64 ± 0.26	0.29 ± 0.05	0.86 ± 0.12	0.61 ± 0.26	0.37 ± 0.06

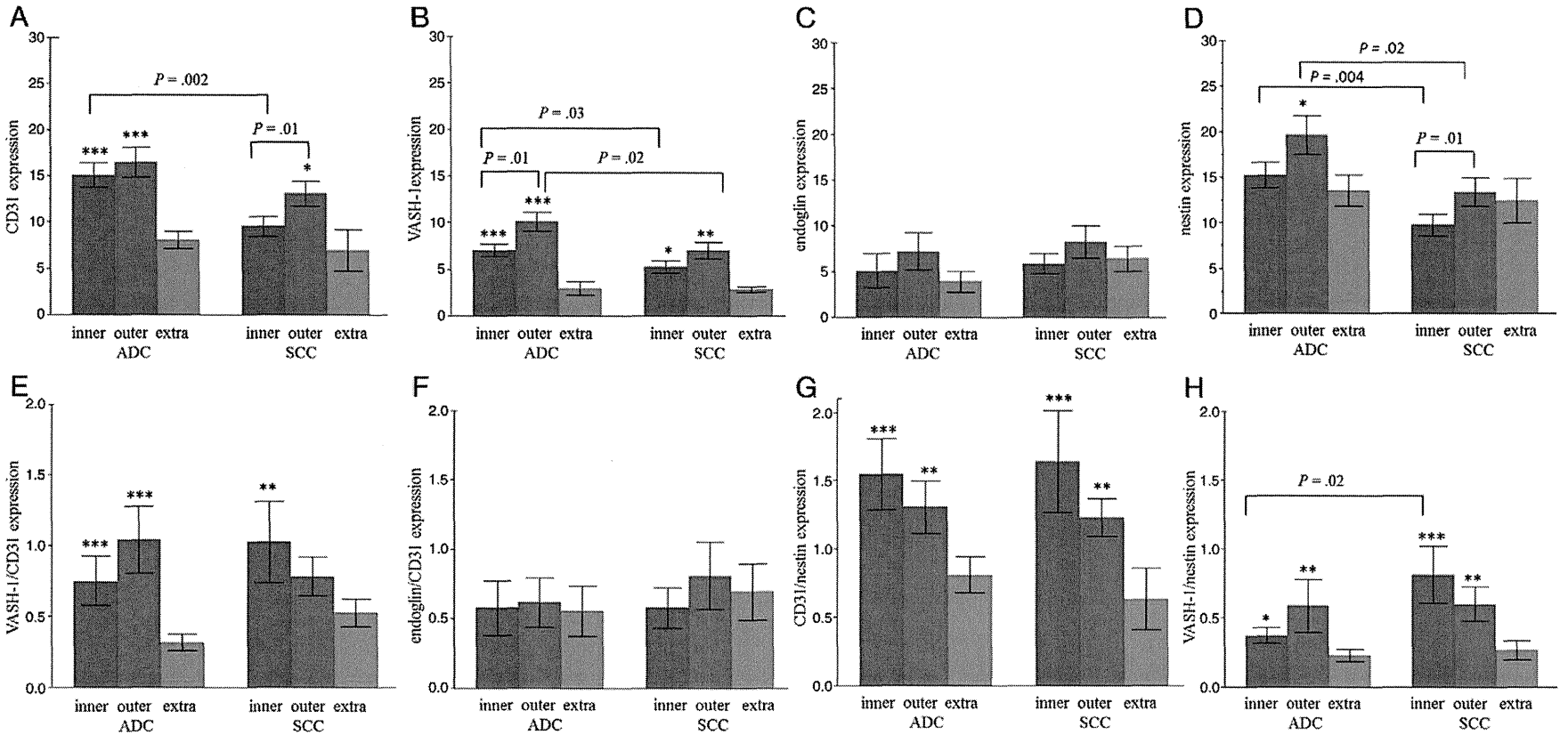

Fig. 2 Summary of the results of immunohistochemistry in ADC and SCC in inner, outer, and extratumoral areas. Mean expression of CD31 (A), VASH-1 (B), endoglin (C), nestin (D), VASH-1/CD31-positive ratio (E), endoglin/CD31 (F), CD31/nestin (G), and VASH-1/nestin (H). The significant difference of the inner and outer areas from the extratumoral area was defined by the following: $*P < .05$, $**P < .01$, and $***P < .001$. Standard error is defined for each graph. Extratumoral area is summarized as "extra" in graphs.

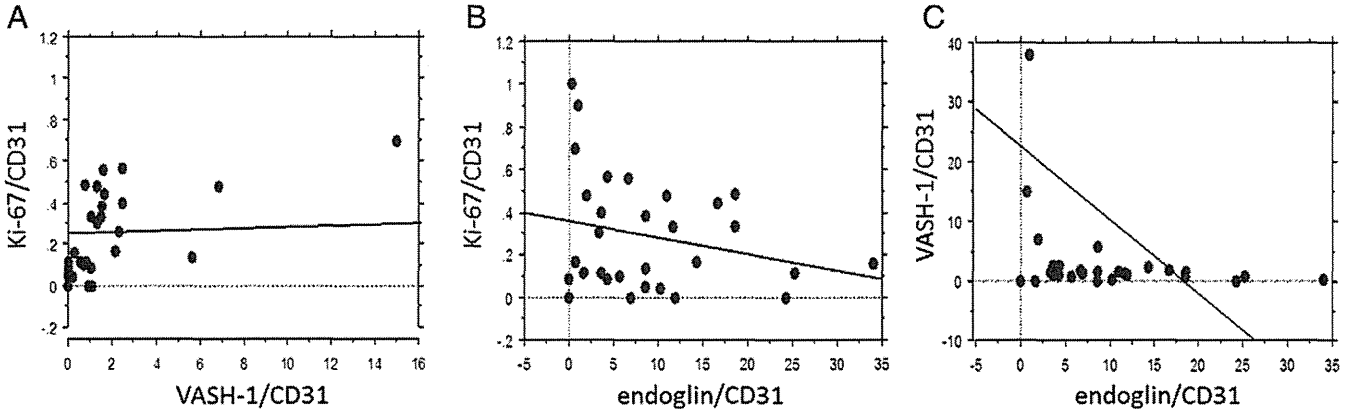

Fig. 3 The correlation between Ki-67 labeling index and VASH-1/CD31 (A) and endoglin/CD31-positive (B) ratios in 30 NSCLC cases examined in our present study (15 ADCs and 15 SCCs), which reveals the significant correlation between Ki-67/CD31 and VASH-1/CD31. C, The correlation between VASH-1/CD31- and endoglin/CD31-positive ratios.

there were no significant differences between inner and outer areas of the tumors examined ($P = .45$). In SCC, the CD31/nestin ratio was also significantly higher in inner ($P > .001$) and outer ($P = .009$) areas of the tumors than in extratumoral areas. The CD31/nestin ratio did not show any significant differences between SCC and ADC in both inner and outer areas ($P = .83$ and $P = .76$, respectively; Fig. 2G). The VASH-1/nestin-positive ratio was also significantly higher in both inner ($P = .03$) and outer ($P = .006$) areas than in extratumoral areas, but there were no significant differences between inner and outer areas in ADC cases ($P = .07$). In SCC cases, the value was also significantly higher in inner ($P > .001$) and outer ($P = .009$) areas of the tumor than in extratumoral area, but not between inner and outer areas ($P = .23$). There were significant differences in VASH-1/nestin ratios in the inner area between ADC and SCC ($P = .02$; Figs. 2H and 5).

3.5. Correlation between clinicopathologic variables and VASH-1/CD31, CD31/nestin, and VASH-1/nestin ratios in intratumoral vessels of NSCLC

The correlation between clinicopathologic variables examined and VASH-1/CD31, CD31/nestin, and VASH-1/nestin ratios in the inner area of the tumor was summarized in Table 3. We studied the correlation in inner areas of the tumor because of the difference in VASH-1/nestin ratios between ADC and SCC, and intratumoral necrosis was usually detected in the inner areas of NSCLC. The necrosis score (%) of the tumor area was significantly correlated with VASH-1/nestin ratio in ADC ($P = .01$).

The VASH-1/nestin ratio in deceased patients was significantly higher than that in living patients in ADC cases ($P = .04$), but not in SCC, whereas a multivariate

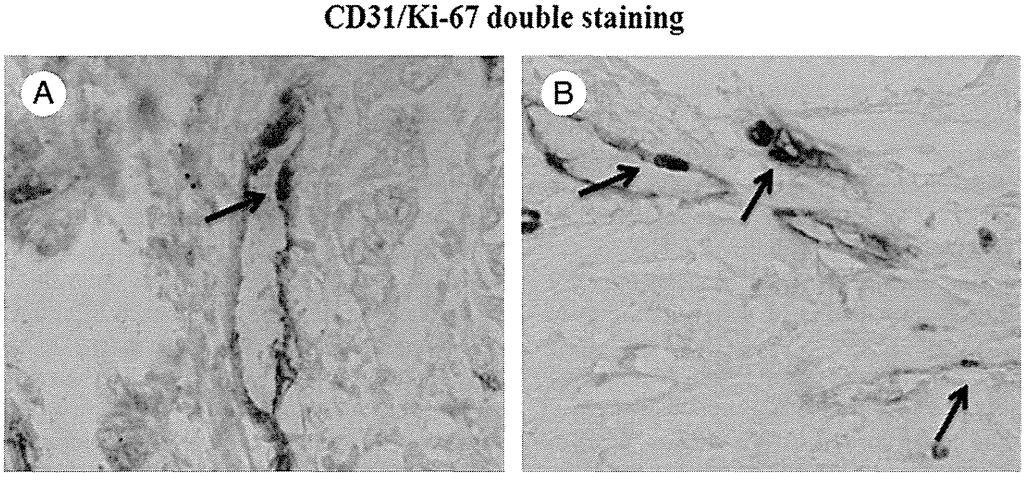

Fig. 4 Double immunostaining for determining proliferating endothelial cells in ADC (A) and SCC (B). Ki-67–positive vessels are illustrated by arrows. CD31 is represented in blue and Ki-67 in brown (×400).

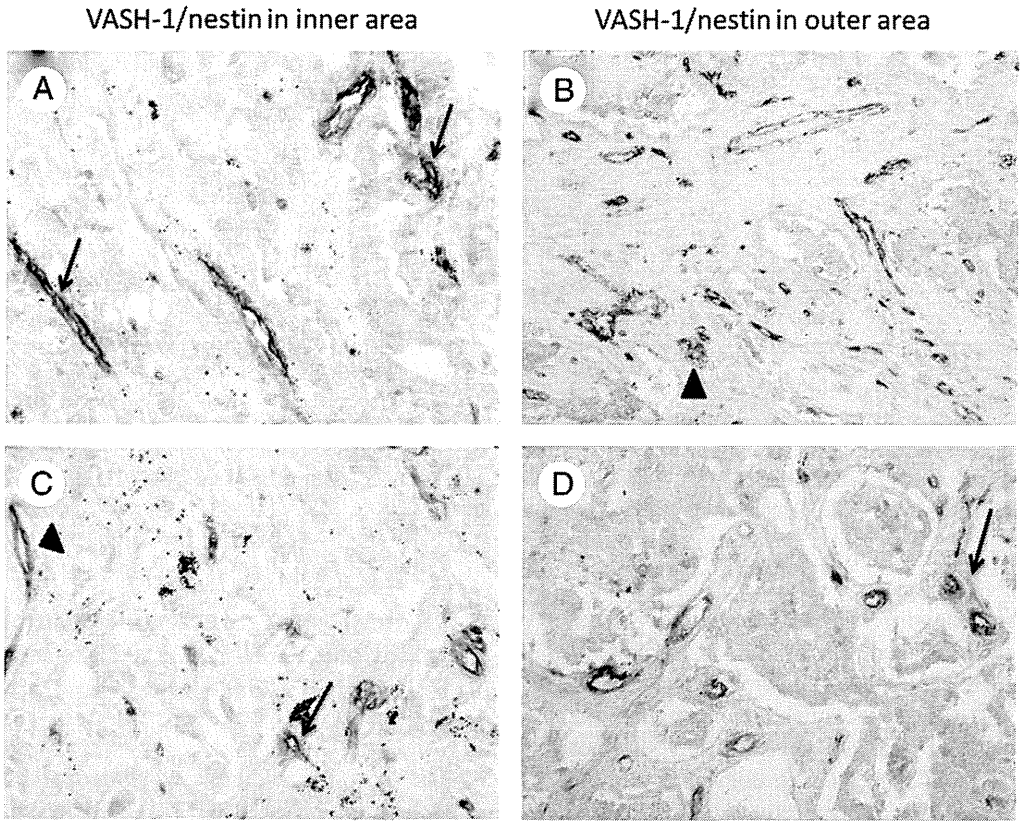

Fig. 5 Representative illustrations of double immunostaining of VASH-1/nestin (A) in the inner area and VASH-1/nestin (B) in the outer area in ADC. VASH-1/nestin (C) in the inner area and VASH-1/nestin (D) in the outer area in SCC. VASH-1 is represented in blue and nestin in brown. Double-positive vessels for VASH-1/nestin were detected both in ADC and in SCC (arrows), and the number of stained vessels only for VASH-1 is defined (arrowheads) (×200).

analysis revealed that histologic type (ADC, SCC; $P = .04$) and VASH-1/nestin ratio ($P = .42$) turned out to be independent prognostic factors. The VASH-1/nestin ratio in poorly differentiated ADC was also significantly higher than that in well- and moderately differentiated ADC cases ($P = .02$).

4. Discussion

In our present study, we evaluated the status of endothelial cells and pericytes in both ADC and SCC to understand the potential differences of the structures of intratumoral vessels between these 2 major histologic subtypes of NSCLC. VASH-1 and endoglin have been studied in some human malignancies but not in NSCLC. In addition, this is the first study to evaluate the status of nestin as an immunohistochemical marker of pericytes in human lung cancer.

The results of our present study did demonstrate significantly higher VASH-1 and CD31 immunoreactivity in both inner and outer areas of the tumor than in extratumoral areas in both ADC and SCC but not endoglin. These results demonstrated that not only high vascularity, as reported previously [16,17], but also neovascularization was more pronounced in tumor areas in the lung. MVD was reported to significantly increase from inner to outer areas in uterine cervical cancer, and a significantly positive correlation was also detected between CD34 level and lymphatic metastases in these patients, which suggested that an induction of angiogenesis could result in an increased potential of metastasis and subsequent adverse clinical outcome of the patients [22]. CD31, one of the most widely used immunohistochemical markers of endothelial cells, has been previously reported to be expressed in both proliferating and resting endothelial cells [23-25]. VASH-1 was, however, demonstrated to be expressed exclusively in proliferating endothelial cells [23]. Tamaki et al [9] proposed the use of the VASH-1/CD31-positive ratio determined by immunohistochemistry as an indicator of neovascularization in breast cancer. In our present study, the overall VASH-1/CD31-positive ratio in ADC was not significantly different from that in SCC but higher in outer than inner areas in both ADC and SCC. In NSCLC, MVD in ADC was also reported to be higher than that in SCC [8,26]. However, our results clearly demonstrated that the number of proliferating vessels was by no means higher in ADC than in SCC. Results of double immunostaining in this study further confirmed the significantly positive correlation between Ki-67–positive proliferating vascular endothelial

Table 3 Association between clinicopathologic variables and VASH-1/CD31, CD31/nestin, and VASH-1/nestin ratios in vessels of 93 NSCLCs

Clinical variables		ADC						SCC					
		VASH-1/CD31-positive ratio	*P*	CD31/nestin-positive ratio	*P*	VASH-1/nestin-positive ratio	*P*	VASH-1/CD31-positive ratio	*P*	CD31/nestin-positive ratio	*P*	VASH-1/nestin-positive ratio	*P*
Stage	I	0.78 ± 0.24		1.53 ± 0.31		0.36 ± 0.07		0.77 ± 0.41		2.13 ± 0.51		0.88 ± 0.30	
	II	0.53 ± 0.75		5.05 ± 2.09		0.38 ± 0.17		2.13 ± 0.76		0.94 ± 1.27		0.12 ± 0.49	
	III	0.96 ± 0.43		0.96 ± 0.69		0.37 ± 0.21		1.01 ± 0.59		1.10 ± 0.77		1.36 ± 0.38	
	IV	1.02 ± 0.21	.22	1.04 ± 0.23	.06	0.42 ± 0.28	.85	2.0 ± 1.87	.46	1.58 ± 0.48	.58	1.92 ± 0.21	.09
Differentiation	Well	0.48 ± 0.29		1.34 ± 0.38		0.25 ± 0.06		0.75 ± 0.42		2.08 ± 0.49		0.57 ± 0.38	
	Moderate	0.93 ± 0.26		3.08 ± 0.80		0.41 ± 0.07		1.40 ± 0.43		1.20 ± 0.70		1.05 ± 0.26	
	Poor	0.96 ± 0.50	.17	1.44 ± 0.41	.38	0.76 ± 0.16	.02*	0.57 ± 0.80	.54	0.86 ± 0.94	.31	0.12 ± 0.61	.08
pT	pT1	1.79 ± 0.27		1.77 ± 0.41		0.21 ± 0.07		0.93 ± 0.60		1.19 ± 0.84		0.86 ± 0.35	
	pT2	1.78 ± 0.34		1.77 ± 0.57		0.56 ± 0.09		1.06 ± 0.39		2.03 ± 0.52		0.5 ± 0.27	
	pT3	0.64 ± 1.32		2.00 ± 1.80		0.59 ± 0.25		1.25 ± 1.90		0.66 ± 2.23		0.92 ± 0.31	
	pT4	1.45 ± 1.32	.25	0.40 ± 1.80	.29	0.72 ± 0.24	.08	1.40 ± 0.95	.73	1.23 ± 1.11	.63	1.92 ± 0.45	.21
pN	pN0	0.73 ± 0.19		1.37 ± 0.27		0.35 ± 0.05		0.79 ± 0.38		2.07 ± 0.48		0.89 ± 0.29	
	pN1	0.53 ± 0.69		3.36 ± 0.90		0.73 ± 0.21		2.29 ± 0.63		0.82 ± 0.97		0.88 ± 0.42	
	pN2	0.99 ± 0.45		1.64 ± 0.90		0.57 ± 0.19		0.55 ± 0.68		1.33 ± 0.97		0.51 ± 0.67	
	pN3		.23		.69		.3	0.76 ± 1.80	.83	1.52 ± 0.54	.46	0.72 ± 0.21	.47
pM	pM0	0.77 ± 0.17		1.56 ± 0.26		0.38 ± 0.05		1.00 ± 0.29		1.64 ± 0.37		0.81 ± 0.20	
	pM1	0.10 ± 1.19	.2	0.95 ± 1.63	.89	0.10 ± 0.27	.32	2.00 ± 1.81	.17	1.25 ± 1.36	.41	1.23 ± 1.42	.52
Survival time	Alive	0.72 ± 0.23		1.58 ± 0.34		0.39 ± 0.22		0.48 ± 0.43		1.10 ± 0.51		0.63 ± 0.33	
	Dead	0.78 ± 0.27	.88	1.53 ± 0.44	.93	1.13 ± 0.28	.04*	1.50 ± 0.39	.09	2.36 ± 0.58	.11	1.41 ± 0.38	.13
Necrosis (%)			.90		.15		.01*		.20		.44		.1

NOTE. Statistical analysis was conducted by Fisher exact test, Wilcoxon rank sum test, and Pearson χ^2 test. The average of VASH-1/CD31, CD31/nestin, and VASH-1/nestin-positive ratio for each clinicopathologic variable is presented. *P* values less than .05 were considered significant and are indicated with an asterisk.

cells and VASH-1–positive endothelial cells, which also indicated that VASH-1 is considered a better marker of neovascularization compared with CD31 in NSCLC, as reported in breast cancer [10]. CD105 or endoglin was also proposed as a highly expressed marker of proliferative tumor vasculature [27], but no significant correlation was detected between endoglin/CD31 and Ki-67/CD31 ratios. Results of our present study were also consistent with those of Eleno et al [28], who reported in uterine paraganglioma that endoglin was exclusively detected in endothelial cells, but Ki-67 had no positive immunoreactivity in these endoglin-positive endothelial cells.

The rapid growth of the tumor is generally considered to result in the insufficient tumor blood supply compared with that required for sustaining the tumor cell proliferation [29]. Bevacizumab was reported to cause central cavity formation in the advanced patients with squamous histology, which was proposed to contribute to the development of intratumoral hemorrhage [29,30]. SCC is the most common lung cancer associated with this central cavity formation [29], but it is also true that the risks of intratumoral hemorrhage after bevacizumab treatment were by no means associated with the development of central cavity formation [29,30]. Formation of pericytes is generally considered as a pivotal step in the process of maturation in newly formed blood vessels [13]. Nestin is one of the most common immunohistochemical markers identifying pericytes [31,15] and has been also used in the analysis of pericytes in intratumoral vessels of pancreatic [32] and colorectal cancers [33]. Our results firstly indicated in lung cancer that the status of nestin immunoreactivity was significantly higher in ADC than in SCC. Results of double immunostaining further demonstrated that the vessels including those newly formed in the tumor microenvironment in ADC were more frequently covered by pericytes than those in SCC. VASH-1–positive vessels in inner areas of tumor in SCC were also demonstrated to be less covered by pericytes than in ADC. These findings all demonstrated that newly formed vessels in SCC, especially those in inner parts of the tumors, were less covered by pericytes. These differences in intratumoral vascular structures between SCC and ADC may also reflect the relative fragility of the vascular wall, which was considered to ultimately increase the risks of intratumoral hemorrhage [13]. Therefore, the relatively higher frequency of lack or absence of pericytes in intratumoral vessels of SCC, especially in newly formed ones, is considered one of the reasons for the increased incidence of intratumoral hemorrhage reported in the patients with SCC after bevacizumab treatment [4]. Results of our present study also demonstrated the significantly positive correlation between intratumoral

necrosis and VASH-1/nestin-positive ratio in ADC, which suggests that the number of newly formed vessels without the concomitant association of pericytes, increases in tumors with higher percentage of necrosis. Tilton et al [34] also reported that the inert basement membrane of the vessels remained intact, forming a tubular scaffold in which regenerating endothelial cells develop to form neovessels after necrosis. Therefore, in ADC, pericytes may also act as a tubular scaffold for neovascular formation after necrosis. In addition, the level of VASH-1/nestin-positive ratio in ADC was higher in deceased patients than in living ones. The number of cases studied was rather small in our present study, but the VASH-1/nestin ratio or the degree of maturation of newly formed intratumoral vessels may serve as a prognostic factor in ADC. However, results of multivariate analysis also demonstrated no significant correlation between VASH-1/nestin ratio and survival in ADC. In addition, pulmonary hemorrhage after the treatment of bevacizumab was mostly detected in patients with clinically advanced inoperable lung cancer [35]. In our present study, none of the patients had received bevacizumab in their clinical course, and further investigations including the correlation between the degrees of angiogenesis/maturation and therapeutic response to bevacizumab are required to establish the relevant targets of bevacizumab in surgical pathology materials of NSCLC cases.

Acknowledgment

We appreciate Kazue Ise (Department of Pathology, Tohoku University School of Medicine) for her skillful technical assistance in double immunohistochemistry despite the enormous damages inflicted upon Tohoku University, Sendai, Japan, by the March 11th earthquake, which interrupted this study.

References

[1] Ryuge S, Sato Y, Wang GQ, et al. Prognostic significance of nestin expression in resected non–small cell lung cancer. Chest 2011;139:862-9.
[2] Yuan Y, Wang F, Liu XH, Gong DJ, Cheng HZ, Huang SD. Angiogenin is involved in lung adenocarcinoma cell proliferation and angiogenesis. Lung Cancer 2009;66:28-36.
[3] Wakelee H. Antibodies to vascular endothelial growth factor in non–small cell lung cancer. J Thorac Oncol 2008;3:113-8.
[4] Di Costanzo F, Mazzoni F, Micol Mela M, Antonuzzo L, Checcacci D, Saggese M. Bevacizumab in non–small cell lung cancer. Drugs 2008; 68:737-46.
[5] Shih T, Lindley C. Bevacizumab: an angiogenesis inhibitor for the treatment of solid malignancies. Clin Ther 2006;28:1779-802.
[6] Manegold C. Bevacizumab for the treatment of advanced non–small-cell lung cancer. Expert Rev Anticancer Ther 2008;8:689-99.
[7] Herbst RS, Sandler A. Bevacizumab and erlotinib: a promising new approach to the treatment of advanced NSCLC. Oncologist 2008;13: 1166-76.
[8] Kojima H, Shijubo N, Abe S. Thymidine phosphorylase and vascular endothelial growth factor in patients with stage I lung adenocarcinoma. Cancer 2002;94:1083-93.
[9] Tamaki K, Moriya T, Sato Y, et al. Vasohibin-1 in human breast carcinoma: a potential negative feedback regulator of angiogenesis. Cancer Sci 2009;100:88-94.
[10] Tamaki K, Sasano H, Maruo Y, et al. Vasohibin-1 as a potential predictor of aggressive behavior of ductal carcinoma in situ of the breast. Cancer Sci 2010;101:1051-8.
[11] de Andrade Santos PP, de Aquino AR, Oliveira Barreto A, de Almeida FR, Galvao HC, de Souza LB. Immunohistochemical expression of nuclear factor kappaB, matrix metalloproteinase 9, and endoglin (CD105) in odontogenic keratocysts, dentigerous cysts, and radicular cysts. Oral Surg Oral Med Oral Pathol Oral Radiol Endod 2011;112: 476-83.
[12] Bergers G, Song S. The role of pericytes in blood-vessel formation and maintenance. Neuro Oncol 2005;7:452-64.
[13] Lu C, Shahzad MM, Moreno-Smith M, et al. Targeting pericytes with a PDGF-B aptamer in human ovarian carcinoma models. Cancer Biol Ther 2010;9:176-82.
[14] Rivera LB, Brekken RA. SPARC promotes pericyte recruitment via inhibition of endoglin-dependent TGF-beta1 activity. J Cell Biol 2011; 193:1305-19.
[15] Nico B, Ennas MG, Crivellato E, et al. Desmin-positive pericytes in the chick embryo chorioallantoic membrane in response to fibroblast growth factor-2. Microvasc Res 2004;68:13-9.
[16] Giatromanolaki A, Koukourakis MI, Sivridis E, O'Byrne K, Gatter KC, Harris AL. 'Invading edge vs. inner' (edvin) patterns of vascularization: an interplay between angiogenic and vascular survival factors defines the clinical behaviour of non–small cell lung cancer. J Pathol 2000;192:140-9.
[17] Giatromanolaki A, Sivridis E, Minopoulos G, et al. Differential assessment of vascular survival ability and tumor angiogenic activity in colorectal cancer. Clin Cancer Res 2000;8:1185-91.
[18] Yatabe Y, Takahashi T, Mitsudomi T. Epidermal growth factor receptor gene amplification is acquired in association with tumor progression of EGFR-mutated lung cancer. Cancer Res 2008;68: 2106-11.
[19] Pyne J, Sapkota D, Wong JC. Aggressive basal cell carcinoma: dermatoscopy vascular features as clues to the diagnosis. Dermatology Practical and Conceptual 2012;2:3-11.
[20] Ito M, Moriya T, Ishida T, et al. Significance of pathological evaluation for lymphatic vessel invasion in invasive breast cancer. Breast Cancer 2007;14:381-7.
[21] Hu CC, Zhang C, Qian Q, Tatum NB. Reparative dentin formation in rat molars after direct pulp capping with growth factors. J Endod 1998; 24:744-51.
[22] Ancuta C, Ancuta E, Zugun-Eloae F, Carasevici E. Neoangiogenesis in cervical cancer: focus on CD34 assessment. Rom J Morphol Embryol 2010;51:289-94.
[23] Hosaka T, Kimura H, Heishi T, et al. Vasohibin-1 expression in endothelium of tumor blood vessels regulates angiogenesis. Am J Pathol 2009;175:430-9.
[24] El Gehani K, Al-Kikhia L, Mansuri N, Syrjanen K, Al-Fituri O, Elzagheid A. Angiogenesis in urinary bladder carcinoma as defined by microvessel density (MVD) after immunohistochemical staining for Factor VIII and CD31. Libyan J Med 2011:6.
[25] Morishita C, Jin E, Kikuchi M, et al. Angiogenic switching in the alveolar capillaries in primary lung adenocarcinoma and squamous cell carcinoma. J Nihon Med Sch 2007;74:344-54.
[26] Shibusa T, Shijubo N, Abe S. Tumor angiogenesis and vascular endothelial growth factor expression in stage I lung adenocarcinoma. Clin Cancer Res 1998;4:1483-7.
[27] Wood LM, Pan ZK, Guirnalda P, Tsai P, Seavey M, Paterson Y. Targeting tumor vasculature with novel *Listeria*-based vaccines directed against CD105. Cancer Immunol Immunother 2011;60: 931-42.
[28] Eleno N, Duwel A, Munoz A, Paz-Bouza J, Lopez-Novoa JM, Lozano F. Endoglin as a marker in cervical paragangliomas. Head Neck 2010; 32:737-43.

[29] Sandler AB, Schiller JH, Gray R, et al. Retrospective evaluation of the clinical and radiographic risk factors associated with severe pulmonary hemorrhage in first-line advanced, unresectable non–small-cell lung cancer treated with carboplatin and paclitaxel plus bevacizumab. J Clin Oncol 2009;27:1405-12.

[30] Marom EM, Martinez CH, Truong MT, et al. Tumor cavitation during therapy with antiangiogenesis agents in patients with lung cancer. J Thorac Oncol 2008;3:351-7.

[31] Alliot F, Rutin J, Leenen PJ, Pessac B. Pericytes and periendothelial cells of brain parenchyma vessels co-express aminopeptidase N, aminopeptidase A, and nestin. J Neurosci Res 1999; 58:367-78.

[32] Kawamoto M, Ishiwata T, Cho K, et al. Nestin expression correlates with nerve and retroperitoneal tissue invasion in pancreatic cancer. HUM PATHOL 2009;40:189-98.

[33] Teranishi N, Naito Z, Ishiwata T, et al. Identification of neovasculature using nestin in colorectal cancer. Int J Oncol 2007;30:593-603.

[34] Tilton RG, Hoffmann PL, Kilo C, Williamson JR. Pericyte degeneration and basement membrane thickening in skeletal muscle capillaries of human diabetics. Diabetes 1981;30:326-34.

[35] Crino L, Dansin E, Garrido P, et al. Safety and efficacy of first-line bevacizumab-based therapy in advanced non-squamous non–small-cell lung cancer (SAiL, MO19390): a phase 4 study. Lancet Oncol 2010;11:733-40.

JCP Online First, published on March 29, 2013 as 10.1136/jclinpath-2013-201444

Vasohibin-1 is a new predictor of disease-free survival in operated patients with renal cell carcinoma

Naoki Kanomata,[1] Yasufumi Sato,[2] Yoshiyuki Miyaji,[3] Atsushi Nagai,[3] Takuya Moriya[1]

[1]Department of Pathology, Kawasaki Medical School, Kurashiki, Okayama, Japan
[2]Department of Vascular Biology, Institute of Development, Aging and Cancer, Tohoku University, Sendai, Japan
[3]Department of Urology, Kawasaki Medical School, Kurashiki, Japan

Correspondence to
Dr Naoki Kanomata, Department of Pathology, Kawasaki Medical School, Matsushima 577, Kurashiki, Okayama 701-0192, Japan; kanomata_7@med.kawasaki-m.ac.jp

Received 4 January 2013
Revised 5 March 2013
Accepted 6 March 2013

ABSTRACT

Background Vasohibin-1 (VASH1) is an endothelium-produced angiogenesis inhibitor. Renal cell carcinoma is highly vascularised, but the significance of endogenous VASH1 in renal cell carcinoma has not been defined.

Aims To identify VASH1 expression and its possible relationship with various clinicopathological factors and prognosis in renal cell carcinoma.

Methods A retrospective analysis of 122 tumours obtained from 118 consecutive patients with renal cell carcinoma was performed. The expression patterns of VASH1, CD31, vascular endothelial growth factor (VEGF) and VEGF receptor type 2 (VEGFR2) were examined immunohistochemically and their relationships with clinicopathological factors were analysed.

Results Microvessel density, VASH1 and VEGFR2 expression were significantly higher in clear cell carcinoma than in other subtypes. The VEGF expression pattern differed significantly between clear cell carcinoma and other histological subtypes. VASH1, pT factor and TNM stage were significantly associated with disease-free survival ($p=0.030$, $p = 0.0012$ and $p = 0.0018$, respectively). Cox models of multivariable disease-free survival analyses indicated that VASH1 and stage are independent prognostic factors ($p=0.019$ and $p = 0.024$).

Conclusions VASH1 expression may be useful for estimating the prognosis of renal cell carcinoma. Further studies of the role of VASH1 in renal cell carcinoma involving larger sample sizes are warranted.

Renal cell carcinoma typically has high vascularity and high histological microvessel density (MVD).[1 2] Angiogenesis is intimately involved in renal cell carcinoma oncogenesis. In clear cell renal cell carcinoma, von Hippel–Lindau gene dysfunction evokes activation of hypoxia-inducible factor (HIF) leading to overexpression of vascular endothelial growth factor (VEGF), angiogenesis acceleration and tumour growth.[3–6] Angiogenesis in the tumour microenvironment is determined by a balance of various stimulatory and inhibitory factors. Angiogenetic factors such as VEGF,[5–10] basic fibroblast growth factor (bFGF),[11 12] thymidine phosphorylase[13 14] and platelet-derived growth factor[15–17] have been studied in renal cell carcinoma; however, the study of natural anti-angiogenic factors in renal cell carcinoma is limited.[18 19]

Vasohibin-1 (VASH1) is an endothelium-derived negative feedback regulator of angiogenesis[20] which regulates endothelial proliferation, migration and lymphangiogenesis.[21] VASH1 expression has been studied in breast cancer,[22 23] uterine cancer[24 25] and cancer of the upper urinary tract[26] but it has not been studied in renal cell carcinoma.

In this study we used immunohistochemistry to examine the expression of VASH1 in renal cell carcinoma and analysed possible relationships between MVD, expression of VEGF and VEGF receptor type 2 (VEGFR2), tumour histology, nuclear grade, vascular invasion, fat invasion and TNM stage. The relationships between VASH1 expression and tumour progression and survival in patients with renal cell carcinoma were also examined.

MATERIALS AND METHODS

A total of 122 tumours obtained from 118 consecutive patients with renal cell carcinoma were reviewed. The samples were obtained from surgical resections performed in the Department of Urology of Kawasaki Medical School, Kurashiki, Japan, from 1986 to 1999.

The paraffin blocks were extracted and thin sections of 5 μm were cut and placed on to Matsunami Adhesive Slide coated glass slides (Matsunami, Osaka, Japan). After deparaffinisation and hydration, hot-bath antigen retrieval was performed at 95°C for 40 min in Target Retrieval Solution, pH 9.0 (Dako, Glostrup, Denmark) for CD31, VASH1 and VEGF, or in citrate buffer, pH 6.0 for VEGFR2. The antibodies used are listed in table 1. The signal was visualised with EnVision Plus (Dako), the chromogen used was 3,3′-diaminobenzidine-tetrachloride and counterstained with haematoxylin for nuclear staining.

The MVD of the tumours was determined by CD31 immunohistochemistry. The densest area ('hot spot') of CD31 reaction was chosen by scanning power and CD31-positive vessels were then counted under a ×20 objective lens (0.785 mm^2, BH-2, Olympus, Tokyo, Japan). The presence of a visible blood vessel lumen was not required for the vessel to be defined as positive. VASH1 and VEGFR2-positive vessels were counted in the same way. The VEGF immunohistochemical pattern was classified as a 'membranous pattern' if the reaction was limited to the cell membrane without cytoplasmic staining or with cytoplasmic staining <10%; 'mixed pattern' if the cytoplasmic staining was 10–90%; and 'cytoplasmic' if the cytoplasmic staining was >90%. One of the authors (NK) evaluated the immunohistochemistry without any knowledge of the patient data.

Statistical analyses were performed using StatView V.5.0 (SAS Institute, Cary, North Carolina, USA) and SPSS Statistics V.19 (IBM, Armonk, New York, USA). The χ^2 test, Fisher exact test and Mann–Whitney test were used to identify

To cite: Kanomata N, Sato Y, Miyaji Y, *et al. J Clin Pathol* Published Online First: [*please include* Day Month Year] doi:10.1136/jclinpath-2013-201444

Table 1 Antibody list

Antigen	Clone	Supplier	Dilution	Incubation
CD31	JC70A	Dako, Glostrup, Denmark	1 : 50	30 min at room temperature
VASH1	(raised against the synthetic fragment Gly286–Arg299 of human VASH1)[20]		2 μg/ml	30 min at room temperature
VEGF	JH121	Lab Vision Co. Fremont, California, USA	1 : 100	Overnight at 4°C
VEGFR2 (Flk-1)	sc-6251	Santa Cruz Biotechnology, Inc, Santa Cruz, California, USA	1 : 100	30 min at room temperature

VASH1, vasohibin-1; VEGF, vascular endothelial growth factor; VEGFR2, vascular endothelial growth factor receptor type 2.

significant differences in the frequencies of the clinicopathological factors and immunohistochemical results. Survival curves were drawn using the Kaplan–Meier method and the differences were assessed by the log-rank test. We also used univariate and multivariable analyses with the Cox proportional hazard regression model to analyse the predictive power of VASH1 expression and other clinicopathological factors in tumour disease-free survival. A p value <0.05 was considered significant.

RESULTS

Characteristic of patients

The patients comprised 79 men and 39 women whose ages ranged from 37 to 85 years (median 56 years). Of the total 122 tumours, 110 tumours were unilateral single tumours and 12 were bilateral and/or multiple tumours. The tumour histology was as follows: 90 clear cell carcinoma (73.8%), 17 chromophobe carcinoma (13.9%), 6 papillary carcinoma (4.9%), 4 acquired cystic disease-associated renal cell carcinoma (3.3%), 1 mucinous tubular and spindle cell carcinoma (0.8%), 1 tubulocystic carcinoma (0.8%) and 3 unclassified carcinoma (2.5%) (figure 1A,B). Fuhrman's nuclear grades were as follows: G1, 2 tumours (1.6%); G2, 34 tumours (27.9%); G3, 72 tumours (59.0%); G4, 14 tumours (11.5%).

The distribution of pT factors according to the Union for International Cancer Control 7th edition were as follows: pT1a, 44 tumours (36.1%); pT1b, 28 tumours (23.0%); pT2a, 17 tumours (13.9%); pT2b, 3 tumours (2.5%); pT3a, 25 tumours (20.5%); pT3b, 4 tumours (3.3%); pT3c, 1 tumour (0.8%). The pN factors were: pN0 or cN0/pNx, 112 tumours (91.8%); pN1, 7 tumours (5.7%); pN2, 3 tumours (2.5%). Nine cases (7.3%) had had distant metastasis at the time of operation. The stages were: stage I, 70 cases (57.4%); stage II, 17 cases (13.9%); stage III, 25 cases (20.5%); stage IV, 10 cases (8.2%).

The treatment comprised radical nephrectomy in 106 tumours (86.9%) and nephron-sparing surgery in 16 tumours (13.1%). The prognostic data were available for 89 of the 110 unilateral single tumours. The follow-up period was 20–7834 days (median 3026). Tumour recurrence occurred in 24 patients. Eighteen patients died from renal cancer and three died of other diseases.

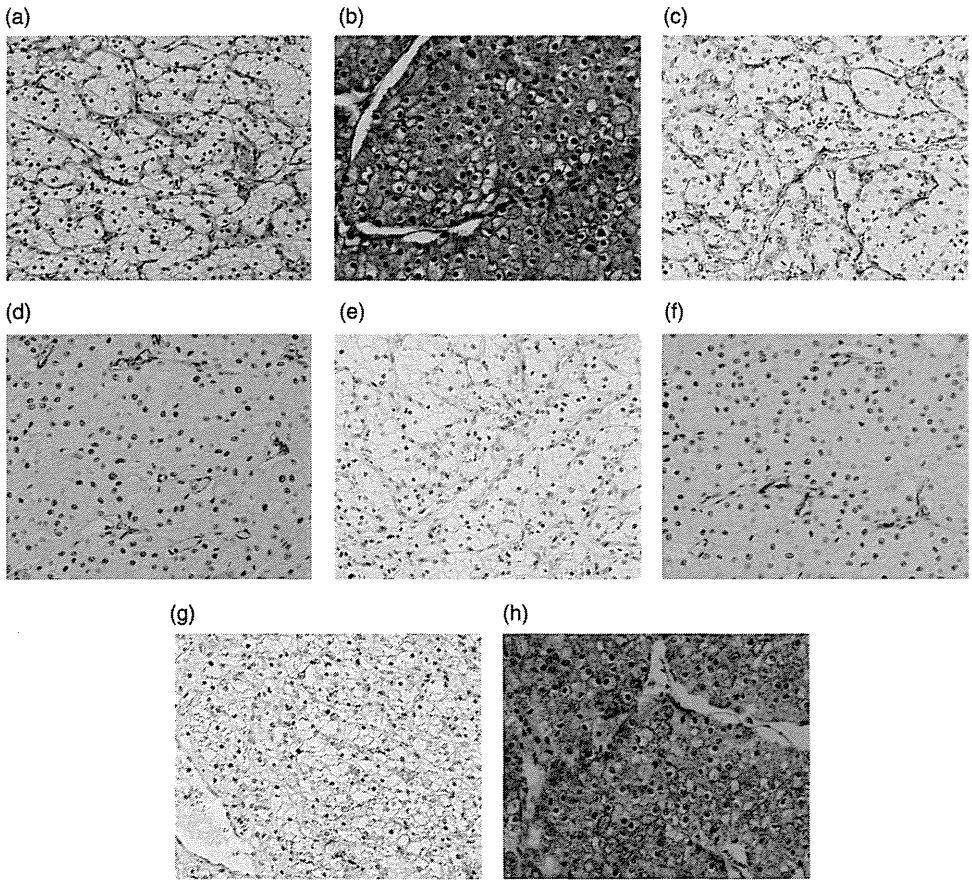

Figure 1 (A, C, E and G) Clear cell renal cell carcinoma; (B, D, F and H) chromophobe renal cell carcinoma. (A and B) H&E staining. (C and D) Immunohistochemical staining of CD31. (E and F) Immunohistochemical staining of vasohibin-1. (G and H) Immunohistochemical staining of vascular endothelial growth factor; membranous pattern (G) and cytoplasmic pattern (H).

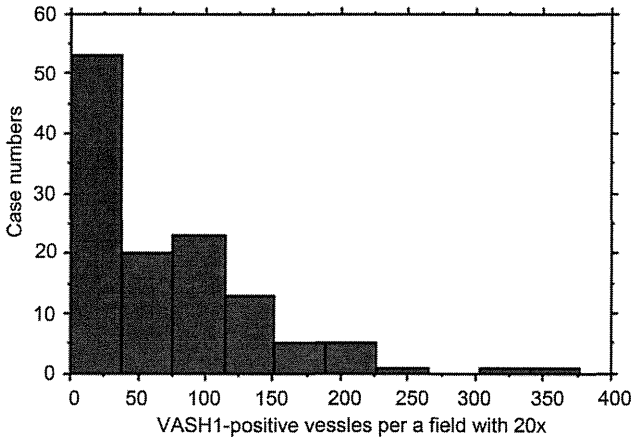

Figure 2 Vasohibin-1 (VASH1) expression of renal cell carcinoma showing a bimodal distribution.

Immunohistochemistry

The tumour MVD was 17–484 per field (median 177), corresponding to 21.7–616.6/mm^2 (median 225.5; figure 1C,D). The number of VASH1-positive vessels ranged from 0 to 378 per field (median 52), corresponding to 0–481.5/mm^2 (median 66.2; figures 1E,F and 2). The number of VEGFR2-positive vessels ranged from 0 to 116 per field (median 6), corresponding to 0–147.8/mm^2 (median 7.6). VEGF immunostaining was classified as membranous in 64 tumours, of mixed pattern in 7 tumours and cytoplasmic in 51 tumours (figure 1G,H).

The comparisons of VASH1 expression and various clinicopathological factors are shown in table 2. The number of VASH1-positive vessels showed a vague bimodal distribution (figure 2), and the cut-off value was set at 95 per field for χ^2 test and Fisher exact test analyses (t=14.42, p<0.0001). VASH1 expression was significantly associated with tumour histology (p<0.0001), MVD (CD31 staining; p<0.0001) and VEGFR2 (p=0.0006). By contrast, VASH1 was not associated with age (p=0.5334), sex (p=0.3886), pT factor (p=0.3714), pN factor (p=0.4319), distant metastasis (p=0.7076), vascular invasion (macroscopically and/or microscopically; p=0.5081), fat invasion (extrarenal and/or renal sinus; p=0.0558) or Fuhrman's nuclear grade (p>0.999) at the cut-off level of 95 per field for VASH1. VASH1 expression was significantly lower in tumours with fat invasion than in those without fat invasion (Mann–Whitney test, p=0.0074).

The MVD (p<0.0001) and expression levels of VASH1 (p<0.0001), VEGFR2 (p<0.0001), VASH1/CD31 (p=0.0079) and VEGFR2/CD31 (p<0.0001) were significantly higher in clear cell renal cell carcinoma than in other subtypes. The expression pattern of VEGF differed significantly between clear cell carcinoma and other subtypes (p=0.0001; table 3).

Among 122 tumours, overall survival could be analysed for 89 of the 110 patients with a unilateral single tumour. By Kaplan–Meier analysis, overall survival was significantly related

Table 2 Comparison of VASH1 and clinicopathological factors

	Low VASH1	High VASH1	p Value
Sex			
Men	52	21	0.3886
Women	23	14	
pT factor			
T1 or T2	62	30	0.3714
T3	23	7	
pN factor			
N0	68	34	0.4319
N1 or N2	7	1	
Distant metastasis			
M0	70	32	0.7076
M1	5	3	
TNM stage			
I or II	52	26	0.6575
III or IV	23	9	
Tumour histology			
Clear cell RCC	54	36	<0.0001*
Others	31	1	
Vascular invasion (macro and/or micro)			
Absent	61	29	0.5081
Present	24	8	
Fat invasion			
Absent	68	35	0.0558
Present	17	2	
	Median (average±SD)	Median (average±SD)	
Age	61 (60.71±11.08)	63 (62.51±10.51)	0.5334
Fuhrman's nuclear grade	3 (2.85±0.627)	3 (2.81±0.569)	>0.999
Microvessel density (CD31)	139 (163.74±94.66)	273 (268.89±65.75)	<0.0001*
VEGFR2	4 (11.41±22.49)	13 (15.86±16.55)	0.0006*

*p<0.05.
RCC, renal cell carcinoma; VASH1, vasohibin-1.